Bräuer, K., Kämpf, H., Strauch, G. (2014): Seismically triggered anomalies in the isotope signatures of mantle-derived gases detected at degassing sites along two neighboring faults in NW Bohemia, central Europe. - *Journal of Geophysical Research*, *119*, 7, p. 5613-5632

DOI: http://doi.org/10.1002/2014JB011044

AGU PUBLICATIONS

JGR

Journal of Geophysical Research: Solid Earth

RESEARCH ARTICLE
10.1002/2014JB011044

Key Points:
- Isotope anomalies detected in gases from different faults after earthquakes
- A pre-seismic increase in 3He/4He (> 6 Ra) indicates magma ascent from mantle
- Isotope monitoring is an excellent way to track active geodynamic processes

Correspondence to:
K. Bräuer,
karin.braeuer@ufz.de

Citation:
Bräuer, K., H. Kämpf, and G. Strauch (2014), Seismically triggered anomalies in the isotope signatures of mantle-derived gases detected at degassing sites along two neighboring faults in NW Bohemia, central Europe, *J. Geophys. Res. Solid Earth*, *119*, 5613–5632, doi:10.1002/2014JB011044.

Received 14 FEB 2014
Accepted 18 JUN 2014
Accepted article online 24 JUN 2014
Published online 10 JUL 2014

Seismically triggered anomalies in the isotope signatures of mantle-derived gases detected at degassing sites along two neighboring faults in NW Bohemia, central Europe

Karin Bräuer[1], Horst Kämpf[2], and Gerhard Strauch[1]

[1]UFZ-Helmholtz Centre for Environmental Research, Halle, Germany, [2]GFZ Helmholtz Centre Potsdam, German Research Centre for Geosciences, Potsdam, Germany

Abstract The Vogtland and NW Bohemia region is known for its earthquake swarms; the most intensive swarm since 1985/86 occurred in October 2008. To find further indications for the interaction of ascending mantle-derived fluids and the occurrence of earthquake swarms, detailed fortnightly studies of gas compositions (CO_2, N_2, Ar, He, H_2, and CH_4) and isotope ratios ($\delta^{13}C$, $\delta^{15}N$, and $^3He/^4He$) were carried out between October 2008 and April 2011 at four locations close to the Nový Kostel focal zone and at the Wettinquelle spring (Bad Brambach). From the start of the 2008 earthquake swarm seismically induced isotope-geochemical anomalies were recorded at locations along the Počatky-Plesná fault zone (PPZ) and were, for the first time, also found at degassing locations on the Mariánské Lázně fault zone (MLF). Variations were observed in both the temporal and spatial distributions of the anomalies as well in anomaly strengths, probably due to the positions of these fault zones relative to the focal zone, and to differences in fluid migration pathways. Prior to both the 2000 and 2008 swarms, $^3He/^4He$ ratios > 6 Ra were recorded at the Bublák mofette. These anomalous pre-seismic $^3He/^4He$ ratios suggest that both the 2000 and 2008 swarms may have been associated with the supply of fresh magma from a less degassed reservoir in the lithospheric mantle. The temporal $\delta^{13}C_{CO2}$ pattern from detailed studies at Bublák between 2005 and 2011 indicates progressive magma degassing, as well as seismically induced variations in the $\delta^{13}C$, providing additional support to the interpretation derived from the $^3He/^4He$ ratios.

1. Introduction

The Vogtland and NW Bohemia region has been host to the most intense earthquake swarms in central Europe. In earthquake swarms the seismic energy is released through a sequence of numerous small- to medium-sized events at shallow focal depths, with no distinct main shock. Earthquake swarms in this region have been well documented since the 19th century [*Credner*, 1876; *Knett*, 1899]. They are generally known from volcanically active areas [e.g., *Hill*, 1977; *Sigmundsson et al.*, 1997; *Schlindwein*, 2012] where they indicate an increase in volcanic activity, but they also occur in areas with no active volcanism, where they are associated with deep-reaching zones of weakness in continental rifts [*Ibs-von Seht et al.*, 2008].

A number of publications in the early 1980s pointed out a connection between the common occurrence of deep-seated fluids (mostly CO_2 discharges) and seismicity [e.g., *Irwin and Barnes*, 1980; *Gold and Soter*, 1984]. Since that time geochemical surveys undertaken in conjunction with geophysical monitoring have contributed to an improved understanding of the complex geodynamic processes triggering seismicity. Anomalies in the compositions and isotope ratios of CO_2-rich gas exhalations have been recorded before, during, and after seismic events. The observed anomalies may reflect a seismically induced release of fluids and/or changes in fluid migration pathways [e.g., *Sugisaki and Sugiura*, 1986; *Tsunogai and Wakita*, 1995; *Hilton*, 1996; *Sano et al.*, 1998; *Toutain and Baubron*, 1999; *Gulec et al.*, 2002; *Caracausi et al.*, 2005; *Chiodini et al.*, 2011].

The mantle-derived fluids escaping in Vogtland and NW Bohemia have been studied in detail for more than 20 years [e.g., *Weinlich et al.*, 1999; *Geissler et al.*, 2005], including their relationships to various strong earthquake swarms that have occurred during that time [e.g., *Bräuer et al.*, 2003, 2008, 2011].

Fischer et al. [2014] have summarized the current state of knowledge concerning earthquake swarms in the Vogtland and NW Bohemia region. The previously assumed association between the migration of pressurized

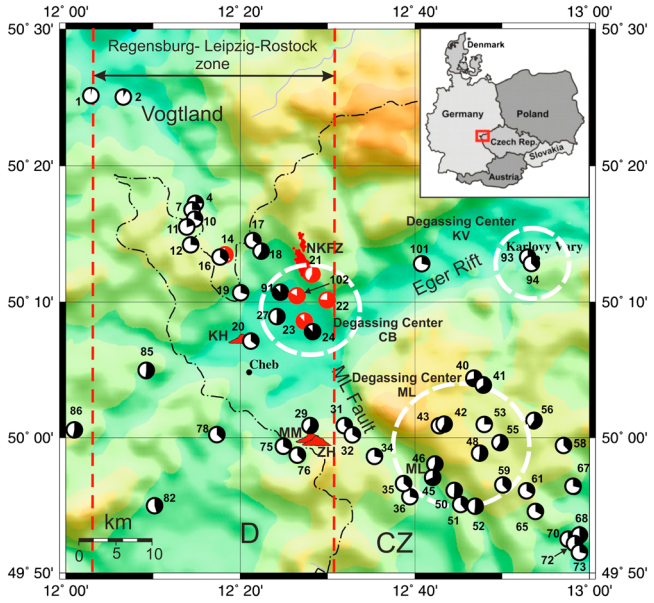

Figure 1. Topographic map of NW Bohemia/Vogtland (modified from *Fischer et al.* [2014]) shows the distribution of degassing locations. The small numbers identify the degassing locations according to *Geissler et al.* [2005]. The quarter circles represent the portions of mantle-derived helium relating to a subcontinental mantle reservoir ($^3He/^4He \approx 6.5$ Ra; *Gautheron et al.* [2005]). The red filled circles mark the position of the monitoring locations. The data were derived from *Weinlich et al.* [1999], *Geissler et al.* [2005], and *Bräuer et al.* [2011]. (NK = Nový Kostel focal zone; CB = Cheb Basin; ML = Mariánské Lázně; KV = Karlovy Vary). The red dots correspond to the hypocenters of the 2008 earthquake swarm, and the red triangles to volcanoes (KH = Komorní hůrka; ZH = Železná hůrka; MM = Mýtina Maar). The Regensburg-Leipzig-Rostock zone [*Bankwitz et al.*, 2003] comprises a number of seismically active N-S trending faults. The inset shows the location of the investigation area within central Europe.

mantle-derived CO_2-rich fluids and the occurrence of earthquake swarms in this region has been confirmed, but further detailed interdisciplinary studies are required if a thorough understanding of the processes involved is to be achieved. This region provides an ideal natural laboratory in which to study fundamental processes that trigger earthquake swarms.

We present new time series data of gas and isotope compositions relevant to the strong earthquake swarm of October 2008, with the data having been collected from four locations close to the Nový Kostel focal zone, and from the Wettinquelle spring, Bad Brambach, about 10 km from the focal zone. To our knowledge this is the first time that degassing locations associated with two different fault zones (the PPZ and the MLF) have been monitored simultaneously.

2. Geological and Seismological Settings

NW Bohemia is located within the transition zone of Saxothuringian, Teplá-Barrandian, and Moldanubian—as triple junction of three separated Variscan structural units [*Babuška et al.*, 2007]. These units were reactivated in the Early Triassic and remain active to the present day. Magmatic activity during the Cenozoic is believed to have been associated with the evolution of the Eger Rift, part of the European Cenozoic Rift System [*Ziegler*, 1992].

The area of investigation is located in the crossing area of the Eger Rift and the Regensburg-Leipzig-Rostock tectonic zone (Figure 1) [*Bankwitz et al.*, 2003]. This tectonic zone comprises several fault zones, of which the MLF and the PPZ are the most important in the Cheb Basin (Figure 2).

Only two small Quaternary volcanoes are known in this area, situated on the flanks of the Eger Rift [*Proft*, 1894]; a maar structure has also been recently identified close to the Železná hůrka scoria cone [*Mrlina et al.*, 2009; Figure 1].

Seismological investigations using receiver functions to search for lithospheric discontinuities [*Geissler et al.*, 2005; *Heuer et al.*, 2006] have revealed crustal thinning from about 31 km to 27 km beneath the western Eger Rift.

Active and passive seismic investigations have yielded a range of Moho depths due to the different resolutions of the methods used and general uncertainties in the Vp/Vs ratios. *Hrubcová and Geissler* [2009] approached this problem by modeling receiver functions and inferred a gradational zone over about 5 km, rather than a sharp discontinuity. Further detailed studies by *Hrubcová et al.* [2013] supported the interpretation of a laminated Moho structure, with a Moho transition zone that varied between 2 and 4 km in thickness at depths ranging from 27 to 31.5 km. Seismic data from the BOHEMA experiment, together with data from previous seismic experiments, have been used to investigate the structure of the upper mantle beneath NW Bohemia [*Heuer et al.*, 2011] and confirmed updoming in the Moho [*Geissler et al.*, 2005]. As a

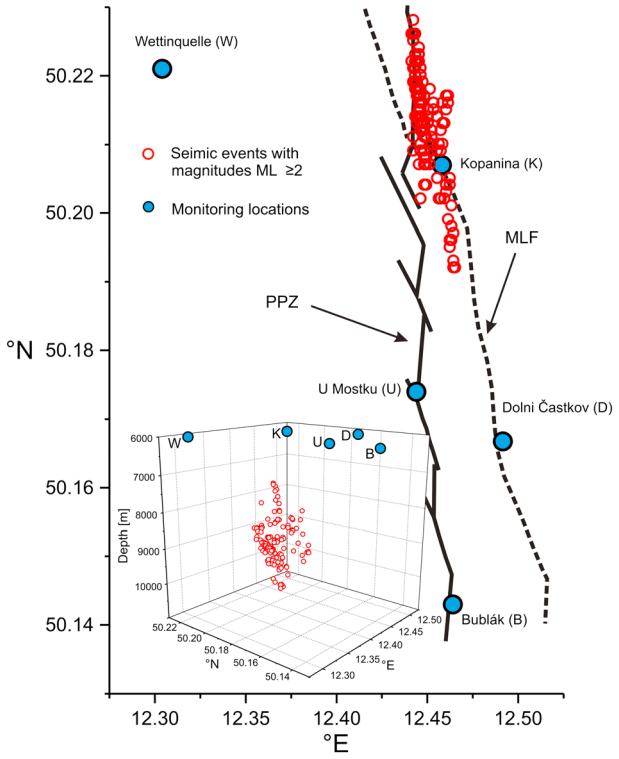

Figure 2. Distribution of foci from the 2008 swarm with $M_L > 2$ (data from the website of the Geophysical Institute in Prague, Academy of Sciences of the Czech Republic: http://www.ig.cas.cz), showing the monitoring locations and the major faults PPZ [after *Bankwitz et al*., 2003] and MLF. The inset shows the spatial distributions of the events with $M_L > 2$.

result the authors concluded that a plume-like structure exists in the upper mantle beneath the western Bohemia earthquake region but that it leaves little or no imprint on the 410 km seismic discontinuity.

Seismic activity since the strong earthquake swarm in 1985/1986 has been recorded in detail by the WEBNET network [*Horálek et al*., 1996]. The first basic information on the 2008 earthquake swarm was published by *Horálek et al*. [2009]; the published data tracked the development of the swarm activity with respect to time as well as the magnitude and location of the swarm events, and also provided a comparison with previous swarms. The main part of the 2008 swarm lasted 23 days and was exceptional in its intensity and rapidity. A more detailed evaluation of the 2008 swarm was later provided by *Fischer et al*. [2010]. Comparisons with previous swarms indicated that the total seismic moments released during the 1985/86 and 2008 swarms were similar, representing the two largest swarms since the 1908 swarm ($M_L \sim 5.0$) in the Vogtland/NW Bohemia region. A comparison of the 2000 and 2008 swarms revealed that the hypocenters of both swarms lay on the same fault section within the Nový Kostel focal zone, at depths of between 6 and 11 km. Besides that an overall upward migration of activity was observed (Figure 3). *Hainzl et al*. [2012] compared the properties of the 2000 and 2008 swarms and studied the migration pattern in greater detail, estimating an underlying change in fluid pressure of up to 30 MPa.

3. Sampling and Methods

Samples were collected every 2 weeks from five locations that had previously (between May 2005 and June 2008) been investigated on a monthly basis [*Bräuer et al*., 2011]. These locations are shown as red circles in Figure 1: Wettinquelle (14), Kopanina (21), Dolni Častkov (22), Bublák (23), and U Mostku (102). Samples were only collected from the free gas phase, using vessels made of AR glass as this type of glass has very low helium permeability. The glass vessels were filled with spring water prior to sampling and the gas bubbles collected with a funnel so that they replaced the water in the vessel. Duplicate samples were generally collected: one sample was used to measure the gas composition and the second was split for isotope analysis (C, He, and N_2). The CO_2 concentration was determined volumetrically, with a precision of 0.1 ml for samples of between 500 and 2000 ml. The other components such as N_2, O_2, Ar, He, H_2, and CH_4 were measured by gas chromatography following CO_2 absorption in KOH solution; the precision was ± 3% for the major components of the residual gas (N_2 and O_2) and ± 10–40% for the minor components (He, Ar, H_2, and CH_4) [*Weinlich et al*., 1998]. The detection limit was < 100 ppm for He and H_2 and < 1 ppm for methane.

It was not possible to carry out air corrections on samples collected from mineral springs because the oxygen concentrations were lower than would normally expected for dissolved air, and argon and neon isotope ratios were not monitored. The only exceptions were at the mofettes; the gas compositions from Bublák and Dolni Častkov (Figure 4) were corrected assuming oxygen stems completely from dissolved air, although variable small amounts of excess air were identified in the Bublák gas [*Bräuer et al*., 2004]. The temperature-

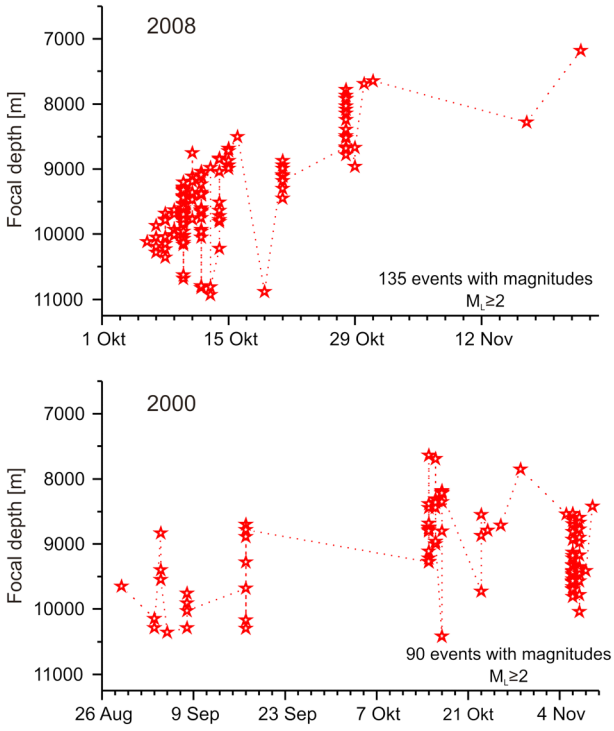

Figure 3. Comparison of the migration patterns (temporal depth-distribution) of seismic events with magnitudes ≥ 2 from the earthquake swarms of 2000 and 2008 (data from the website of the Geophysical Institute in Prague, Academy of Sciences of the Czech Republic: http://www.ig.cas.cz).

dependent N_2/O_2 and Ar/O_2 ratios were used to calculate the proportions of nitrogen and argon derived from air.

For $\delta^{13}C$ analyses, CO_2 and water were separated from the non-condensable gases by two-step cryogenic separation in a vacuum, at liquid nitrogen temperature. Water vapor was retained by a mixture of dry ice and alcohol at −78°C. The isotopic analysis of carbon was carried out using a Thermo-Finnigan Delta V Plus mass spectrometer, and the $\delta^{13}C$ values (determined relative to PDB) were reproducible to < 0.1‰.

The small fraction of non-condensable gas was split and filled into AR glass ampoules, which were sealed and later used for analysis to determine the isotope ratios of nitrogen and helium. The $\delta^{15}N$ values were determined relative to an air nitrogen standard, and their reproducibility was ± 0.2‰. Following each isotope measurement a mass scan was carried out in which the intensities of the mass 32 and mass 40 peaks were monitored in order to check for the possible introduction of atmospheric contamination during sample handling. The mass 44 peak was also checked to monitor the CO_2/N_2 separation procedure and to evaluate any inaccuracies that might have occurred in the $\delta^{15}N$ values due to CO forming from partial cracking of residual CO_2 on the hot electron-emitting filament during the measurements [*Bräuer et al.*, 2004].

In order to analyze the $^3He/^4He$ ratios the second AR glass ampoule was connected to a fully automated noble gas mass spectrometer system equipped with a two-stage cryo-system. Helium and neon were separated from other gases in the first cryo-trap, at a temperature of 25K. A split was then analyzed for $^4He/^{20}Ne$ using a sensitive quadrupole mass spectrometer. The remaining He and Ne were transferred to a second cryo-trap at a temperature of 14K, where the gases were adsorbed onto activated charcoal. Through precise temperature control the helium was then desorbed at 45K and transferred to a dedicated sector field mass spectrometer in which ^3He was separated from HD molecules; the ^3He was then detected using a Channeltron electron multiplier and ^4He using a Faraday cup [*Sültenfuß et al.*, 2009].

4. Results

In order to monitor the 2008 earthquake swarm samples were analyzed from October 2008 to April 2011. The complete record of field data, gas compositions, and isotope ratios ($\delta^{13}C_{CO2}$, $\delta^{15}N_{N2}$, and $^3He/^4He$) is presented in Table 1. The field data indicate different water characteristic at each location. In the Cheb Basin the gas percolated through water with only low levels of mineralization, whereas at the Wettinquelle spring the gas had interacted with mineralized water that it passed through prior to sampling. Due to the low pH values and low conductivities at the Cheb Basin locations, the effect of bicarbonate was not relevant.

4.1. Gas Composition

The major gas component at all monitoring locations was CO_2. The admixture of dissolved air with mantle-derived gas needs to be taken into account because the gas percolated through water before sampling. However, carbon dioxide, helium, and methane should be little affected by the admixture of dissolved air

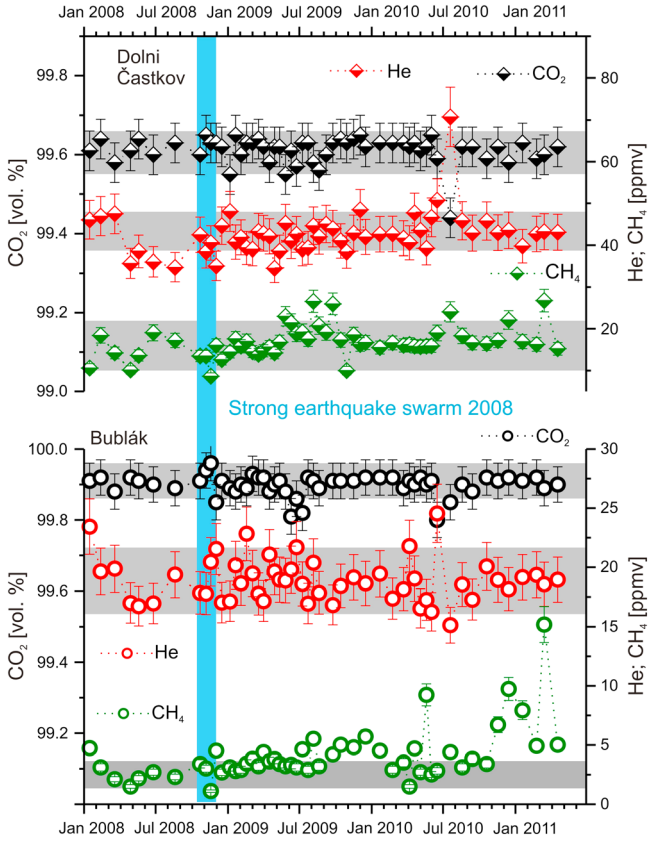

Figure 4. Variations in the non-atmospheric gas components (CO_2, He, and CH_4) of two gas-rich mofettes (Bublák in the PPZ and Dolni Častkov in the MLF) relating to the strong earthquake swarm of 2008. The blue bars represent the duration of the swarm. The gray bars correspond to the range of values in time of seismic quiescence [after *Bräuer et al.*, 2011], and the error bars represent 2σ.

because of their low atmospheric concentrations. Seasonal variations in CO_2 concentrations were observed at all springs due to the strong temperature-dependence of CO_2 solubility. The greatest variations in CO_2 concentration were observed at both of the low mineralized springs (U Mostku and Kopanina, Table 1) in the Cheb Basin, due to their low gas/water ratios [*Bräuer et al.*, 2011]. Because this effect was not evident at the mofettes (Bublák and Dolni Častkov), only the time series of the (predominantly geogenic) components from these locations (carbon dioxide, helium, and methane) are shown in Figure 4 (air corrected gas compositions). The CO_2 concentration in the gas from Bublák was a little higher than that in the gas from Dolni Častkov. After the beginning of the seismically active period repeatedly anomalies of the CO_2 concentration were observed at both mofettes; also, helium and methane showed clear anomalies.

Hydrogen was detectable at the Wettinquelle and Bublák for several months beginning in the early 2009 (Table 1), as had also previously been noted from the time series studies carried out before, during, and after the seismically active period in 2000. During periods of seismic quiescence the hydrogen concentration was mostly below the limit of detection (~100 ppm) following CO_2 absorption in KOH solution [*Bräuer et al.*, 2008].

The methane concentration also increased sporadically at all monitored locations (Figure 5) following the start of the seismically active period, relative to the average values from periods of seismic quiescence [*Bräuer et al.*, 2011].

4.2. Isotopic Compositions

The isotope signatures of the analyzed gases differed markedly between the various monitoring locations (Table 1). The variations in $^3He/^4He$ ratios and $\delta^{13}C$ values during periods of seismic quiescence were small [*Bräuer et al.*, 2011], but the range in $\delta^{15}N$ values was greater due to the admixture of varying proportions of dissolved air.

At least modified by solubility effects are the $^3He/^4He$ ratios (Figure 6). The two component crust-mantle mixing procedure resulted in distinctly elevated proportions of mantle-derived helium at the monitored locations (ranging from approximately 38% at Wettinquelle to 93% at Bublák), based on a subcontinental mantle helium isotope signature of 6.32 ± 0.39 Ra [*Gautheron et al.*, 2005]. Compared to the mean values (gray bars), the time series clearly show greater variations from the start of the seismically active period than during the pre-seismic period, at all monitored locations in the Cheb Basin (Figure 6) and at Wettinquelle (Table 1 and Figure 8a). A repeated overall decrease in the $^3He/^4He$ ratios over a period of about 2 years following the start of the earthquake swarm was observed at all monitored locations. The shifts were more marked at the mofettes than at the springs, and more marked at the locations along the MLF (Dolni Častkov and Kopanina) than at those along the PPZ (Bublák and U Mostku).

Table 1. Recorded Data Due to 2008 Earthquake Swarm[a]

		Field Data			Gas Composition							Isotope Data		
		ϑ_{H2O}	Cond.	pH	CO_2	He	H_2	O_2	N_2	Ar	CH_4	$\delta^{13}C$	$\delta^{15}N$	$^3He/^4He$
			µS/cm	°C	vol.%	ppmv	ppmv	vol.%	vol.%	vol.%	ppmv	‰	‰	Ra
Wettinquelle	11.10.2008	11.6	1738	5.68	99.75	2.2	b.d.l.	0.018	0.23	0.005	31.8	−4.69	2.6	2.36
Wettinquelle	21.10.2008	11.6	1721	5.66	99.73	1.6	b.d.l.	0.019	0.24	0.006	24.2	−4.70	2.8	2.39
Wettinquelle	06.11.2008	11.6	1642	5.57	99.68	1.9	b.d.l.	0.025	0.29	0.007	35.6	−4.72	−0.7	2.43
Wettinquelle	18.11.2008	11.5	1700	5.95	99.79	1.2	b.d.l.	0.016	0.19	0.004	13.7	−4.71	0.1	2.39
Wettinquelle	02.12.2008	11.5	1702	6.08	99.75	1.1	b.d.l.	0.019	0.23	0.006	20.2	−4.63	3.2	2.41
Wettinquelle	16.12.2008	11.2	1742	5.76	99.76	1.4	b.d.l.	0.009	0.22	0.005	25.8	−4.71	1.5	2.32
Wettinquelle	06.01.2009	11.1	1705	5.89	99.77	1.6	b.d.l.	0.012	0.21	0.005	22.2	−4.69	0.1	2.38
Wettinquelle	20.01.2009	11.4	1802	5.95	99.80	1.3	0.8	0.012	0.18	0.004	27.1	−4.72	−0.2	2.39
Wettinquelle	03.02.2009	10.9	1779	6.13	99.82	1.3	0.4	0.014	0.16	0.004	20.8	−4.65	0.6	2.40
Wettinquelle	17.02.2009	10.7	1763	6.31	99.80	1.9	0.4	0.014	0.18	0.004	21.2	−4.71	1.5	2.58
Wettinquelle	04.03.2009	10.3	1772	5.76	99.60	2.3	1.8	0.023	0.37	0.008	41.4	−4.80	1.1	n.d.
Wettinquelle	19.03.2009	10.6	1741	5.74	99.45	3.7	0.9	0.021	0.51	0.012	64.6	−4.69	1.1	2.35
Wettinquelle	01.04.2009	9.8	1743	5.78	99.56	3.6	1.1	0.015	0.41	0.010	65.9	−4.79	1.2	2.39
Wettinquelle	16.04.2009	9.7	1780	5.76	99.65	2.0	1.0	0.011	0.32	0.008	35.9	−4.80	1.4	2.39
Wettinquelle	29.04.2009	9.7	1778	5.59	99.66	2.1	0.6	0.016	0.31	0.008	37.3	−4.82	1.1	2.38
Wettinquelle	12.05.2009	10.0	1760	5.77	99.60	2.7	0.5	0.015	0.37	0.008	38.9	−4.78	1.0	2.31
Wettinquelle	27.05.2009	10.0	1755	5.75	99.70	2.3	0.0	0.014	0.27	0.007	27.2	−4.79	3.5	n.d.
Wettinquelle	10.06.2009	10.5	1796	5.73	99.76	1.5	0.3	0.011	0.22	0.006	21.7	−4.78	2.4	2.45
Wettinquelle	24.06.2009	10.4	1809	5.82	99.71	1.7	0.3	0.019	0.26	0.006	22.7	−4.77	2.2	2.65
Wettinquelle	09.07.2009	10.9	1836	5.83	99.84	1.9	0.3	0.006	0.15	0.005	17.5	−4.78	1.9	2.39
Wettinquelle	23.07.2009	11.3	1837	5.77	99.82	2.0	0.2	0.010	0.16	0.004	18.2	−4.74	4.2	2.66
Wettinquelle	06.08.2009	11.3	1854	5.77	99.85	1.3	0.2	0.009	0.13	0.003	17.1	−4.79	2.2	2.44
Wettinquelle	20.08.2009	11.2	1865	5.81	99.84	1.1	0.3	0.017	0.14	0.004	17.0	−4.75	1.9	2.39
Wettinquelle	07.09.2009	11.2	1868	5.76	99.86	0.9	0.1	0.009	0.12	0.003	18.7	−4.67	0.7	2.40
Wettinquelle	24.09.2009	12.0	1850	5.62	99.85	1.3	0.5	0.011	0.13	0.003	19.5	−4.74	1.7	2.46
Wettinquelle	14.10.2009	11.8	n.d.	5.82	99.84	1.2	0.7	0.010	0.15	0.004	22.6	−4.74	2.2	2.59
Wettinquelle	29.10.2009	11.9	1816	5.82	99.82	1.4	0.8	0.016	0.16	0.004	24.4	−4.77	2.8	2.48
Wettinquelle	16.11.2009	11.9	1805	5.80	99.82	1.2	0.2	0.013	0.16	0.004	22.1	−4.72	2.3	2.46
Wettinquelle	03.12.2009	11.8	1830	5.80	n.d.	n.d.	n.d.	n.d.	n.d.	n.d.	n.d.	−4.66	−0.6	2.44
Wettinquelle	16.12.2009	11.6	1806	5.86	99.83	1.6	b.d.l.	0.007	0.16	0.004	26.0	−4.77	1.0	2.38
Wettinquelle	22.01.2010	11.5	1828	5.84	99.85	1.2	b.d.l.	0.009	0.13	0.003	48.3	−4.73	0.9	2.24
Wettinquelle	23.02.2010	11.2	1881	5.86	99.61	1.6	b.d.l.	0.059	0.32	0.005	47.1	−4.73	−0.4	2.36
Wettinquelle	23.03.2010	10.6	1773	5.78	99.62	2.0	b.d.l.	0.019	0.35	0.009	60.8	−4.69	0.5	n.d.
Wettinquelle	07.04.2010	10.4	1783	5.73	99.74	2.1	b.d.l.	0.008	0.24	0.006	36.4	−4.85	0.3	2.37
Wettinquelle	20.04.2010	10.2	1803	5.81	99.77	1.9	b.d.l.	0.012	0.20	0.006	33.2	−4.82	0.2	2.35
Wettinquelle	05.05.2010	10.3	1824	5.84	99.79	1.8	b.d.l.	0.007	0.20	0.005	21.9	−4.80	1.9	2.35
Wettinquelle	20.05.2010	10.3	1811	5.83	99.77	1.2	b.d.l.	0.015	0.20	0.005	36.7	−4.74	−0.1	2.25
Wettinquelle	02.06.2010	10.6	1820	5.81	99.81	1.5	b.d.l.	0.010	0.17	0.004	18.6	−4.89	1.1	2.33
Wettinquelle	16.06.2010	10.8	1819	5.85	99.80	1.1	b.d.l.	0.015	0.18	0.005	19.7	−4.80	3.1	2.38
Wettinquelle	20.07.2010	11.5	1845	5.88	99.88	1.0	0.1	0.007	0.11	0.003	21.1	−4.78	0.6	2.40
Wettinquelle	19.08.2010	11.1	1768	5.81	99.77	1.8	0.8	0.008	0.22	0.005	41.5	−4.81	0.2	2.39
Wettinquelle	14.09.2010	11.6	1789	5.82	99.84	1.4	0.2	0.008	0.15	0.004	24.5	−4.83	0.7	2.35
Wettinquelle	20.10.2010	11.6	1830	5.88	99.85	1.3	0.1	0.010	0.13	0.003	18.4	−4.77	1.5	2.39
Wettinquelle	18.11.2010	11.4	1785	5.85	99.77	1.6	0.9	0.007	0.21	0.005	43.0	−4.71	1.4	2.40
Bublák	19.08.2008	13.3	104	4.37	99.48	19.3	b.d.l.	0.138	0.36	0.012	2.3	−2.10	−2.4	5.91
Bublák	22.10.2008	9.2	118	4.51	99.65	17.8	b.d.l.	0.088	0.25	0.008	3.4	−2.12	−2.4	5.86
Bublák	06.11.2008	8.7	116	4.42	99.51	17.7	b.d.l.	0.148	0.33	0.011	3.0	−2.09	−2.3	5.94
Bublák	18.11.2008	6.7	120	4.64	99.20	20.3	b.d.l.	0.264	0.51	0.019	1.1	−2.02	−1.6	5.92
Bublák	02.12.2008	4.9	121	4.58	99.18	21.4	b.d.l.	0.235	0.57	0.013	4.5	−2.08	−1.5	5.90
Bublák	16.12.2008	5.4	122	4.40	99.76	17.0	b.d.l.	0.052	0.18	0.004	2.7	−2.13	−1.2	5.89
Bublák	06.01.2009	0.8	119	4.54	99.65	17.1	b.d.l.	0.082	0.26	0.005	3.1	−1.95	−1.4	5.95
Bublák	20.01.2009	1.9	298	4.45	99.52	20.1	b.d.l.	0.126	0.34	0.008	2.8	−2.02	−2.8	5.89
Bublák	03.02.2009	3.8	117	n.d.	99.56	18.6	5.2	0.118	0.31	0.007	2.9	−2.01	−1.6	5.94
Bublák	17.02.2009	2.8	123	n.d.	99.34	22.7	3.7	0.191	0.45	0.010	3.4	−1.97	−0.9	5.91
Bublák	04.03.2009	5.7	128	4.71	99.52	19.4	1.4	0.144	0.33	0.008	3.8	−2.01	0.0	5.78
Bublák	19.03.2009	6.4	114	n.d.	99.57	17.7	2.5	0.125	0.30	0.008	3.2	−2.06	−1.5	5.91
Bublák	01.04.2009	7.8	123	4.66	99.60	17.1	0.5	0.112	0.28	0.007	4.4	−2.02	−1.1	5.88
Bublák	16.04.2009	11.9	111	4.65	99.49	21.0	0.9	0.135	0.36	0.009	3.6	−2.04	−2.4	n.d.
Bublák	29.04.2009	10.6	113	4.61	99.66	19.6	b.d.l.	0.084	0.25	0.007	3.8	−2.10	−1.9	5.88

Table 1. (continued)

		Field Data			Gas Composition							Isotope Data		
		ϑ_{H2O}	Cond.	pH	CO_2	He	H_2	O_2	N_2	Ar	CH_4	$\delta^{13}C$	$\delta^{15}N$	$^3He/^4He$
			µS/cm	°C	vol.%	ppmv	ppmv	vol.%	vol.%	vol.%	ppmv	‰	‰	Ra
Bublák	12.05.2009	11.6	110	4.66	99.57	18.9	b.d.l.	0.115	0.30	0.007	3.4	−2.04	−1.9	5.85
Bublák	27.05.2009	12.8	106	4.62	99.39	18.8	b.d.l.	0.170	0.43	0.009	3.2	−1.99	−1.3	5.89
Bublák	10.06.2009	12.0	110	4.61	99.27	19.7	b.d.l.	0.189	0.53	0.011	3.3	−2.13	0.5	5.81
Bublák	24.06.2009	11.8	113	4.63	99.46	21.6	b.d.l.	0.135	0.39	0.008	3.1	−2.17	−1.9	5.93
Bublák	09.07.2009	12.8	106	4.66	99.22	18.5	b.d.l.	0.210	0.56	0.011	4.6	−2.13	−2.3	5.90
Bublák	23.07.2009	13.4	105	4.61	99.62	16.9	1.4	0.104	0.27	0.007	2.9	−2.02	−3.0	5.91
Bublák	06.08.2009	14.3	107	4.59	99.54	20.3	b.d.l.	0.127	0.32	0.008	5.5	−2.18	0.0	5.90
Bublák	20.08.2009	12.7	128	4.50	99.60	17.8	b.d.l.	0.102	0.29	0.007	3.2	−2.10	0.8	5.85
Bublák	07.09.2009	12.7	128	4.50	n.d.	n.d.	b.d.l.	n.d.	n.d.	n.d.	n.d.	−2.14	−2.1	5.92
Bublák	24.09.2009	12.4	132	4.48	99.72	16.8	b.d.l.	0.065	0.21	0.005	4.2	−2.16	−2.9	5.86
Bublák	14.10.2009	8.7	n.d.	4.67	99.69	18.4	b.d.l.	0.079	0.23	0.006	5.0	−2.13	−1.9	5.91
Bublák	29.10.2009	9.2	131	4.60	n.d.	n.d.	b.d.l.	n.d.	n.d.	n.d.	n.d.	−2.14	−1.0	5.65
Bublák	16.11.2009	7.7	128	4.67	99.62	19.1	b.d.l.	0.103	0.27	0.007	4.8	−2.15	−2.6	5.94
Bublák	03.12.2009	6.2	130	4.60	n.d.	n.d.	b.d.l.	n.d.	n.d.	n.d.	n.d.	−2.07	−1.4	5.88
Bublák	16.12.2009	3.6	137	4.62	99.69	18.6	b.d.l.	0.078	0.22	0.006	5.7	−2.08	−2.6	5.92
Bublák	22.01.2010	4.9	102	4.56	99.60	19.4	b.d.l.	0.111	0.28	0.007	4.5	−2.08	−1.8	5.85
Bublák	23.02.2010	4.2	149	4.65	99.58	17.3	b.d.l.	0.120	0.30	0.006	2.9	−2.09	−2.2	5.91
Bublák	23.03.2010	7.3	157	4.71	99.56	18.1	b.d.l.	0.118	0.32	0.008	3.5	−2.09	−1.5	5.89
Bublák	07.04.2010	8.9	138	4.70	99.51	21.7	b.d.l.	0.137	0.34	0.008	1.5	−2.13	−1.4	5.57
Bublák	20.04.2010	10.4	134	4.71	99.61	19.0	b.d.l.	0.099	0.28	0.007	4.7	−2.09	−1.6	5.96
Bublák	05.05.2010	9.8	135	4.68	99.67	16.5	b.d.l.	0.088	0.24	0.005	2.7	−2.15	−2.1	5.87
Bublák	20.05.2010	9.4	138	4.76	99.54	17.2	b.d.l.	0.125	0.33	0.007	9.2	−2.06	−2.5	5.95
Bublák	02.06.2010	10.1	127	4.72	99.62	16.2	b.d.l.	0.099	0.27	0.006	2.5	−2.22	−1.9	5.90
Bublák	16.06.2010	13.3	121	4.35	99.16	24.4	b.d.l.	0.224	0.61	0.013	2.8	−2.02	−2.1	5.96
Bublák	20.07.2010	14.7	150	n.d.	99.67	15.1	b.d.l.	0.062	0.26	0.006	4.4	−2.19	−0.7	5.94
Bublák	19.08.2010	12.5	116	4.64	99.64	18.5	b.d.l.	0.090	0.26	0.006	3.1	−2.24	−1.4	5.93
Bublák	14.09.2010	10.9	109	4.65	99.44	17.2	b.d.l.	0.152	0.40	0.010	3.8	−2.11	−2.1	5.97
Bublák	20.10.2010	7.8	119	4.63	99.54	20.0	b.d.l.	0.133	0.32	0.009	3.4	−2.13	−0.8	5.89
Bublák	18.11.2010	7.8	119	4.59	99.71	18.9	b.d.l.	0.066	0.21	0.005	6.7	−2.12	−1.3	n.d.
Bublák	15.12.2010	7.8	119	4.59	99.61	18.1	b.d.l.	0.105	0.27	0.006	9.7	−2.06	−2.2	5.67
Bublák	19.01.2011	5.7	117	4.48	99.56	19.1	b.d.l.	0.122	0.31	0.007	7.9	−2.03	−0.3	5.79
Bublák	24.02.2011	2.7	120	4.50	99.54	19.3	b.d.l.	0.135	0.32	0.007	4.9	−2.03	−1.7	5.67
Bublák	15.03.2011	6.6	121	4.51	99.46	18.5	b.d.l.	0.152	0.38	0.009	15.1	−2.14	−1.5	5.95
Bublák	19.04.2011	10.1	128	4.49	99.58	18.9	b.d.l.	0.112	0.30	0.007	5.0	−2.13	1.0	5.94
U Mostku	19.08.2008	11.9	100	4.48	82.69	75	b.d.l.	0.915	16.0	0.358	80	−0.79	0.3	5.60
U Mostku	22.10.2008	9.2	96	4.60	89.20	53	b.d.l.	0.238	10.3	0.232	152	−0.79	0.4	5.66
U Mostku	06.11.2008	9.5	97	4.45	85.91	69	b.d.l.	0.852	12.9	0.294	126	−0.98	0.8	5.56
U Mostku	18.11.2008	7.7	93	4.57	86.47	56	b.d.l.	0.867	12.4	0.293	71	−1.02	0.5	5.61
U Mostku	02.12.2009	7.4	95	4.51	86.27	59	b.d.l.	0.801	12.6	0.358	90	−1.19	0.8	5.62
U Mostku	16.12.2009	7.5	100	4.23	88.59	67	b.d.l.	0.294	10.8	0.260	10	−1.22	0.6	5.62
U Mostku	06.01.2009	5.8	98	4.53	87.23	73	b.d.l.	0.217	12.2	0.285	219	−1.29	0.7	5.63
U Mostku	20.01.2009	6.7	100	4.15	n.d.	n.d.	b.d.l.	n.d.	n.d.	n.d.	n.d.	−1.15	0.7	5.60
U Mostku	03.02.2009	6.4	99	n.d.	84.29	99	18.9	0.349	15.0	0.288	123	−1.10	0.2	5.59
U Mostku	17.02.2009	4.1	95	n.d.	71.02	188	b.d.l.	1.539	26.8	0.545	368	−0.94	0.5	5.58
U Mostku	04.03.2009	6.3	108	4.53	87.26	136	b.d.l.	0.132	12.3	0.291	440	−1.07	1.0	5.63
U Mostku	19.03.2009	7.9	n.d.	n.d.	85.08	96	b.d.l.	0.426	14.1	0.328	456	−0.88	0.7	5.62
U Mostku	01.04.2009	7.0	102	4.42	85.39	119	b.d.l.	0.490	13.8	0.325	252	−1.09	0.4	5.60
U Mostku	16.04.2009	8.8	101	4.39	69.52	125	b.d.l.	4.358	25.7	0.445	94	−1.22	0.7	5.62
U Mostku	29.04.2009	7.3	107	4.42	84.33	100	b.d.l.	0.493	14.8	0.360	38	−1.06	0.4	5.54
U Mostku	12.05.2009	8.2	103	4.39	85.57	95	b.d.l.	0.278	13.8	0.321	38	−0.98	0.9	5.62
U Mostku	27.05.2009	9.4	104	4.36	83.50	104	b.d.l.	0.379	15.7	0.379	138	−1.14	0.6	5.59
U Mostku	10.06.2009	10.0	105	4.39	69.52	125	b.d.l.	4.358	25.7	0.445	94	−0.91	−0.6	5.61
U Mostku	24.06.2009	10.8	103	4.52	84.33	100	b.d.l.	0.493	14.8	0.360	38	−0.87	0.5	5.61
U Mostku	09.07.2009	10.6	105	4.42	85.57	95	b.d.l.	0.278	13.8	0.321	38	−1.14	0.5	5.60
U Mostku	23.07.2009	11.3	107	4.36	83.50	104	b.d.l.	0.379	15.7	0.379	138	−1.17	0.5	5.57
U Mostku	06.08.2009	12.8	104	3.49	85.45	65	b.d.l.	1.135	13.1	0.326	206	−0.82	0.3	5.60
U Mostku	20.08.2009	13.0	99	4.38	88.22	66	b.d.l.	0.595	10.9	0.298	94	−0.90	−0.1	5.57
U Mostku	07.09.2009	12.5	105	4.40	86.38	66	b.d.l.	1.068	12.2	0.348	246	−1.07	0.6	5.60

Table 1. (continued)

		Field Data			Gas Composition							Isotope Data		
		ϑ_{H2O}	Cond.	pH	CO_2	He	H_2	O_2	N_2	Ar	CH_4	$\delta^{13}C$	$\delta^{15}N$	$^3He/^4He$
			µS/cm	°C	vol.%	ppmv	ppmv	vol.%	vol.%	vol.%	ppmv	‰	‰	Ra
U Mostku	24.09.2009	12.1	99	4.42	89.36	53	b.d.l.	0.560	9.8	0.298	153	−0.93	0.9	5.55
U Mostku	14.10.2009	9.4	n.d.	4.67	88.38	44	b.d.l.	0.784	10.5	0.284	188	−0.94	0.7	5.50
U Mostku	29.10.2009	10.3	103	4.49	n.d.	n.d.	b.d.l.	n.d.	n.d.	n.d.	n.d.	−1.02	0.7	5.57
U Mostku	16.11.2009	9.3	103	4.50	90.66	39	b.d.l.	0.689	8.4	0.262	307	−1.22	0.4	5.56
U Mostku	03.12.2009	7.6	102	4.46	89.48	44	b.d.l.	0.879	9.3	0.275	171	−0.59	0.6	5.58
U Mostku	16.12.2009	6.5	109	3.91	86.85	48	b.d.l.	1.127	11.7	0.328	236	−0.84	0.0	5.58
U Mostku	22.01.2009	4.9	102	4.56	80.70	58	b.d.l.	0.670	18.2	0.444	137	−0.36	0.1	5.55
U Mostku	23.02.2010	6.8	102	4.44	83.38	98	b.d.l.	0.929	15.3	0.395	147	−0.50	0.1	5.57
U Mostku	23.03.2010	7.6	114	4.78	n.d.	n.d.	b.d.l.	n.d.	n.d.	n.d.	n.d.	−1.17	0.4	5.60
U Mostku	07.04.2010	8.2	112	4.25	82.46	107	b.d.l.	0.979	16.1	0.391	255	−0.56	0.5	5.56
U Mostku	20.04.2010	8.9	138	4.36	81.88	118	b.d.l.	1.058	16.6	0.429	179	−0.76	0.3	5.51
U Mostku	05.05.2010	8.5	108	4.30	81.36	132	b.d.l.	0.759	17.5	0.374	141	−0.82	−0.4	5.51
U Mostku	20.05.2010	8.8	115	4.48	82.50	115	b.d.l.	0.828	16.3	0.388	222	−0.69	−0.3	5.55
U Mostku	02.06.2010	8.4	104	4.46	82.54	71	b.d.l.	1.095	15.9	0.409	217	−0.81	0.0	5.53
U Mostku	16.06.2010	9.6	106	3.95	77.88	70	b.d.l.	1.408	20.2	0.532	51	−0.74	0.0	5.54
U Mostku	20.07.2010	12.9	106	n.d.	83.53	68	b.d.l.	0.990	15.1	0.352	567	−0.70	−0.3	5.64
U Mostku	19.08.2010	11.1	105	4.40	90.66	43	b.d.l.	0.525	8.5	0.242	288	−0.97	0.0	5.62
U Mostku	14.09.2010	10.6	106	4.59	89.87	50	b.d.l.	0.478	9.4	0.263	215	−1.40	0.3	5.61
U Mostku	20.10.2010	9.1	103	4.42	89.34	55	b.d.l.	0.569	9.8	0.296	195	−0.81	0.4	5.55
U Mostku	18.11.2010	8.8	103	4.39	90.67	51	b.d.l.	0.306	8.7	0.258	277	−1.01	0.3	5.61
Kopanina	19.08.2008	10.4	259	4.31	81.92	390	b.d.l.	0.600	17.2	0.286	50.1	−2.11	1.0	4.59
Kopanina	22.10.2008	9.0	244	4.35	81.20	468	b.d.l.	0.735	17.7	0.292	53.8	−1.72	1.0	4.58
Kopanina	06.11.2008	9.3	252	4.48	82.17	414	b.d.l.	0.328	17.2	0.282	55.0	−1.97	1.5	4.63
Kopanina	18.11.2008	8.2	244	4.86	n.d.	n.d.	n.d.	n.d.	n.d.	n.d.	n.d.	−1.81	1.1	4.56
Kopanina	02.12.2009	8.4	248	4.52	n.d.	n.d.	n.d.	n.d.	n.d.	n.d.	n.d.	−2.87	−0.2	4.49
Kopanina	16.12.2009	5.3	246	4.33	n.d.	n.d.	n.d.	n.d.	n.d.	n.d.	n.d.	−2.39	0.9	4.63
Kopanina	06.01.2009	6.6	247	4.69	n.d.	n.d.	n.d.	n.d.	n.d.	n.d.	n.d.	−2.99	0.7	4.60
Kopanina	20.01.2009	7.5	256	4.49	n.d.	n.d.	n.d.	n.d.	n.d.	n.d.	n.d.	−2.02	1.3	4.57
Kopanina	03.02.2009	7.5	253		n.d.	n.d.	n.d.	n.d.	n.d.	n.d.	n.d.	−2.06	0.3	4.50
Kopanina	17.02.2009	7.0	254	4.66	n.d.	n.d.	n.d.	n.d.	n.d.	n.d.	n.d.	−1.71	1.2	4.55
Kopanina	04.03.2009	6.4	261	4.55	72.81	533	b.d.l.	1.331	25.5	0.314	111.2	−1.78	1.2	4.52
Kopanina	19.03.2009	6.5	265	4.71	73.33	705	b.d.l.	1.078	25.2	0.344	98.5	−1.80	1.1	4.51
Kopanina	01.04.2009	6.8	266	4.53	77.74	521	b.d.l.	0.344	21.6	0.281	94.9	−2.04	1.2	4.56
Kopanina	16.04.2009	9.5	267	4.44	78.80	662	b.d.l.	0.713	20.1	0.268	79.5	−2.07	1.1	4.54
Kopanina	29.04.2009	9.3	267	4.54	83.01	422	b.d.l.	0.035	16.7	0.250	87.9	−2.00	1.5	4.55
Kopanina	12.05.2009	10.1	266	4.55	77.47	501	b.d.l.	0.710	21.5	0.275	77.6	−1.82	1.1	4.55
Kopanina	27.05.2009	10.5	292	4.53	80.27	485	b.d.l.	0.406	19.0	0.245	105.0	−1.94	1.2	4.57
Kopanina	10.06.2009	10.2	265	4.50	n.d.	n.d.	n.d.	n.d.	n.d.	n.d.	n.d.	−1.32	n.d.	n.d.
Kopanina	24.06.2009	9.8	261	4.35	83.15	405	b.d.l.	0.250	16.3	0.217	80.7	−2.18	1.0	4.62
Kopanina	09.07.2009	10.2	258	4.43	78.68	339	b.d.l.	2.025	19.0	0.279	79.6	−1.96	1.2	4.61
Kopanina	23.07.2009	12.1	249	4.41	78.47	747	b.d.l.	1.018	20.2	0.269	122.6	−2.08	0.7	4.59
Kopanina	06.08.2009	11.6	259	4.22	82.61	414	b.d.l.	0.730	16.4	0.252	132.8	−2.07	1.0	4.56
Kopanina	20.08.2009	11.5	262	4.19	84.69	333	b.d.l.	0.811	14.2	0.229	96.4	−2.17	1.2	4.56
Kopanina	07.09.2009	10.8	259	4.28	81.58	373	b.d.l.	1.391	16.7	0.251	92.2	−2.13	1.1	4.59
Kopanina	24.09.2009	10.4	264	4.45	81.80	501	b.d.l.	0.975	16.9	0.233	115.4	−1.93	1.3	4.58
Kopanina	14.10.2009	9.4	n.d.	4.67	81.81	461	b.d.l.	0.388	17.5	0.257	76.7	−2.09	1.3	4.59
Kopanina	29.10.2009	8.6	252	4.43	77.65	415	b.d.l.	1.412	20.5	0.380	63.3	−2.12	0.3	4.64
Kopanina	16.11.2009	9.3	103	4.50	79.20	426	b.d.l.	1.149	19.3	0.266	113.2	−1.90	0.9	4.59
Kopanina	03.12.2009	7.6	102	4.46	80.41	674	b.d.l.	0.353	18.9	0.245	103.5	−2.10	0.8	4.56
Kopanina	16.12.2009	6.5	109	3.91	77.40	555	b.d.l.	0.327	21.9	0.313	117.5	−1.89	1.0	4.53
Kopanina	22.01.2009	4.9	102	4.56	77.05	672	b.d.l.	0.258	22.2	0.392	104.3	−1.94	1.1	4.72
Kopanina	23.02.2010	6.8	102	4.44	76.23	782	b.d.l.	0.364	23.0	0.309	106.7	−1.85	1.0	4.62
Kopanina	23.03.2010	7.6	114	4.78	76.34	590	b.d.l.	0.958	22.4	0.281	104.6	n.d.	n.d.	n.d.
Kopanina	07.04.2010	8.2	112	4.25	75.83	784	b.d.l.	0.509	23.3	0.280	105.9	−2.28	0.6	4.61
Kopanina	20.04.2010	8.9	138	4.36	78.21	607	b.d.l.	0.512	20.9	0.283	86.2	−1.98	n.d.	n.d.
Kopanina	05.05.2010	8.4	259	4.45	77.83	598	b.d.l.	0.826	21.0	0.259	100.0	−2.06	1.1	4.53
Kopanina	20.05.2010	8.6	257	4.84	80.08	536	b.d.l.	0.361	19.2	0.261	81.5	−1.84	0.9	4.55
Kopanina	02.06.2010	9.0	253	4.46	80.56	624	b.d.l.	0.270	18.9	0.243	90.8	−1.87	0.5	4.58

Table 1. (continued)

		Field Data			Gas Composition							Isotope Data		
		ϑ_{H2O}	Cond.	pH	CO_2	He	H_2	O_2	N_2	Ar	CH_4	$\delta^{13}C$	$\delta^{15}N$	$^3He/^4He$
			µS/cm	°C	vol.%	ppmv	ppmv	vol.%	vol.%	vol.%	ppmv	‰	‰	Ra
Kopanina	16.06.2010	10.3	256	4.48	81.07	535	b.d.l.	0.346	18.3	0.237	95.3	−2.21	0.6	4.59
Kopanina	20.07.2010	11.4	254	4.41	n.d.	n.d.	b.d.l.	n.d.	n.d.	n.d.	n.d.	−2.12	0.6	4.63
Kopanina	19.08.2010	10.9	256	4.40	84.38	350	b.d.l.	0.176	15.2	0.220	151.0	−2.22	1.2	4.63
Kopanina	14.09.2010	9.7	225	4.41	81.39	583	b.d.l.	0.686	17.5	0.314	157.2	−2.16	0.8	4.66
Kopanina	20.10.2010	8.2	254	4.40	81.63	532	b.d.l.	0.283	17.8	0.242	105.6	n.d.	n.d.	n.d.
Kopanina	18.11.2010	8.3	252	4.38	83.19	467	b.d.l.	0.184	16.3	0.225	115.2	−1.97	0.5	4.62
Kopanina	16.12.2010	n.d.	n.d.	n.d.	79.34	480	b.d.l.	0.381	19.9	0.281	123.9	−1.78	0.3	4.64
Dolni Càstkov	19.08.2008	15.5	236	4.61	99.49	34.7	b.d.l.	0.047	0.45	0.009	17.2	−2.04	0.5	5.19
Dolni Càstkov	22.10.2008	10.4	308	4.79	99.47	42.4	b.d.l.	0.045	0.47	0.009	13.5	−2.03	0.4	5.15
Dolni Càstkov	06.11.2008	9.7	338	4.52	99.58	38.4	b.d.l.	0.025	0.38	0.007	13.5	−1.84	0.6	4.88
Dolni Càstkov	18.11.2008	7.8	412	4.02	99.47	40.5	b.d.l.	0.055	0.46	0.010	8.6	−1.96	−0.2	5.14
Dolni Càstkov	02.12.2009	5.5	315	4.13	99.44	35.0	b.d.l.	0.064	0.48	0.007	16.0	−1.99	0.1	5.17
Dolni Càstkov	16.12.2009	5.2	257	4.23	99.49	44.6	b.d.l.	0.045	0.45	0.008	12.6	−1.88	0.1	5.16
Dolni Càstkov	06.01.2009	0.3	313	4.75	99.17	47.9	b.d.l.	0.136	0.68	0.013	14.4	−1.89	0.2	5.17
Dolni Càstkov	20.01.2009	4.1	115	4.20	99.52	40.7	b.d.l.	0.046	0.42	0.008	17.6	−1.91	0.7	4.93
Dolni Càstkov	03.02.2009	2.4	307	4.51	99.41	41.8	4.8	0.070	0.51	0.009	15.8	−1.85	0.2	5.19
Dolni Càstkov	17.02.2009	1.2	349	4.46	99.44	39.3	3.5	0.065	0.48	0.008	17.0	−1.93	−0.1	5.18
Dolni Càstkov	04.03.2009	3.1	212	4.41	99.44	39.0	3.0	0.067	0.48	0.008	14.5	−1.84	0.1	5.14
Dolni Càstkov	19.03.2009	4.5	n.d.	n.d.	99.50	43.2	b.d.l.	0.049	0.44	0.008	13.9	−2.07	0.1	5.15
Dolni Càstkov	01.04.2009	5.9	231	4.29	99.34	42.7	1.9	0.097	0.55	0.010	14.7	−2.12	0.1	5.14
Dolni Càstkov	16.04.2009	10.8	333	4.13	99.27	42.0	1.6	0.110	0.61	0.011	15.6	−1.98	0.2	5.14
Dolni Càstkov	29.04.2009	10.0	271	4.31	99.50	34.5	b.d.l.	0.045	0.45	0.008	14.2	−1.97	0.6	5.11
Dolni Càstkov	12.05.2009	13.1	262	4.16	99.48	38.5	b.d.l.	0.047	0.46	0.008	16.8	−1.93	0.1	5.15
Dolni Càstkov	27.05.2009	15.4	272	4.76	99.43	45.2	b.d.l.	0.039	0.51	0.009	23.0	−2.00	0.2	5.03
Dolni Càstkov	10.06.2009	14.4	278	4.29	99.43	40.9	b.d.l.	0.059	0.49	0.009	21.4	−1.97	2.0	5.04
Dolni Càstkov	24.06.2009	13.6	282	4.81	99.39	42.5	b.d.l.	0.060	0.53	0.009	18.8	−1.97	1.0	4.91
Dolni Càstkov	09.07.2009	16.1	329	4.97	99.36	38.9	b.d.l.	0.093	0.53	0.010	19.2	−1.94	0.3	5.16
Dolni Càstkov	23.07.2009	15.6	352	5.18	99.42	39.3	b.d.l.	0.073	0.49	0.009	17.5	−2.03	1.6	5.03
Dolni Càstkov	06.08.2009	17.6	248	4.47	99.22	44.5	1.4	0.125	0.64	0.012	26.5	−1.97	0.6	4.82
Dolni Càstkov	20.08.2009	22.2	339	5.38	99.29	41.9	b.d.l.	0.092	0.60	0.012	20.7	−1.94	1.5	4.97
Dolni Càstkov	07.09.2009	18.9	284	5.24	99.22	44.9	b.d.l.	0.129	0.63	0.013	19.1	−1.95	0.9	4.84
Dolni Càstkov	24.09.2009	18.0	251	5.17	99.32	43.8	b.d.l.	0.105	0.55	0.011	25.9	−1.93	2.1	4.93
Dolni Càstkov	14.10.2009	10.2	n.d.	4.91	99.56	41.0	b.d.l.	0.027	0.40	0.007	17.3	−1.94	−0.2	5.14
Dolni Càstkov	29.10.2009	10.4	310	4.47	99.50	38.3	b.d.l.	0.045	0.44	0.008	10.0	−1.99	1.5	4.90
Dolni Càstkov	16.11.2009	8.2	258	4.45	99.46	42.8	b.d.l.	0.061	0.46	0.008	18.5	−1.99	0.7	4.90
Dolni Càstkov	03.12.2009	7.4	257	4.40	99.46	48.4	b.d.l.	0.069	0.46	0.008	16.2	−1.91	1.6	4.96
Dolni Càstkov	16.12.2009	7.4	257	4.40	99.49	41.9	b.d.l.	0.047	0.45	0.008	16.7	−1.91	0.7	4.92
Dolni Càstkov	22.01.2009	4.9	259	4.54	99.39	42.5	b.d.l.	0.083	0.50	0.014	15.5	−1.93	1.7	4.95
Dolni Càstkov	23.02.2010	5.9	259	4.48	99.45	42.6	b.d.l.	0.060	0.47	0.008	16.6	−1.86	−1.3	4.84
Dolni Càstkov	23.03.2010	7.8	256	4.49	99.46	41.6	b.d.l.	0.059	0.47	0.009	16.0	−1.93	1.7	4.82
Dolni Càstkov	07.04.2010	8.0	271	4.33	99.37	40.5	b.d.l.	0.086	0.53	0.010	16.2	−1.95	1.5	4.93
Dolni Càstkov	20.04.2010	8.8	260	4.34	99.39	47.6	b.d.l.	0.082	0.51	0.010	15.8	−1.98	0.8	4.90
Dolni Càstkov	05.05.2010	9.2	329	4.10	99.43	43.5	b.d.l.	0.063	0.49	0.009	15.7	−1.91	1.5	5.00
Dolni Càstkov	20.05.2010	n.d.	315	4.56	99.46	39.2	b.d.l.	0.054	0.47	0.008	15.8	−2.05	1.4	5.08
Dolni Càstkov	02.06.2010	10.7	302	4.13	99.49	46.6	b.d.l.	0.054	0.44	0.008	15.9	−2.00	0.5	4.86
Dolni Càstkov	16.06.2010	15.2	294	3.76	99.41	50.7	b.d.l.	0.061	0.51	0.009	19.0	n.d.	n.d.	n.d.
Dolni Càstkov	20.07.2010	17.7	399	n.d.	99.12	70.5	0.9	0.113	0.75	0.011	24.0	−1.92	1.2	5.04
Dolni Càstkov	19.08.2010	14.9	214	4.32	99.51	45.8	b.d.l.	0.039	0.44	0.007	18.3	−2.05	2.0	5.02
Dolni Càstkov	14.09.2010	13.1	267	4.05	99.42	42.8	b.d.l.	0.068	0.49	0.009	16.6	−2.01	1.9	5.04
Dolni Càstkov	20.10.2010	9.3	396	3.88	99.25	45.6	b.d.l.	0.118	0.61	0.013	16.4	−2.03	0.0	4.81
Dolni Càstkov	18.11.2010	7.8	243	4.09	99.46	42.9	b.d.l.	0.054	0.47	0.010	17.2	−2.05	0.0	5.19
Dolni Càstkov	15.12.2010	0.5	118	4.66	99.46	43.5	b.d.l.	0.043	0.48	0.009	22.1	−1.89	0.0	5.20
Dolni Càstkov	19.01.2011	3.6	268	3.88	99.48	39.7	b.d.l.	0.052	0.45	0.008	16.9	−1.89	0.5	5.14
Dolni Càstkov	24.02.2011	1.6	366	4.00	99.37	42.6	b.d.l.	0.076	0.54	0.009	16.2	−1.95	0.6	5.18
Dolni Càstkov	15.03.2011	5.3	427	3.79	99.35	43.1	b.d.l.	0.090	0.55	0.010	26.7	−1.99	1.0	n.d.
Dolni Částkov	19.04.2011	6.1	531	3.66	99.41	43.0	b.d.l.	0.070	0.50	0.009	15.2	−1.84	1.6	4.96

[a] n.d. = not determined. b.d.l. = below detection limit. The Bublák $\delta^{13}C$ values correspond to the mean of two samples.

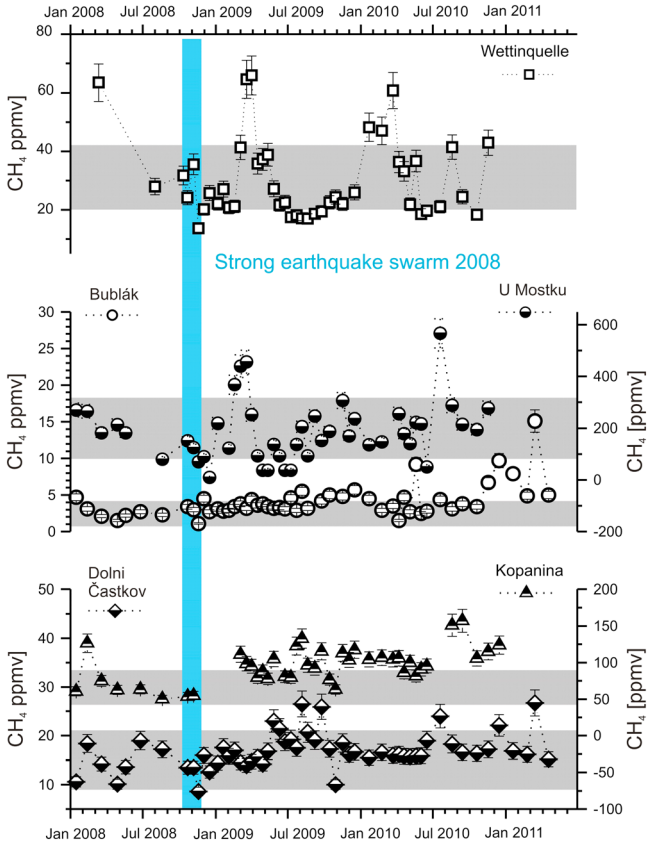

Figure 5. Comparison of the methane monitoring pattern of all locations. The blue bars represent the duration of the swarm. The gray bars correspond to the range of values in time of seismic quiescence [after *Bräuer et al.*, 2011], and the error bars represent 2σ.

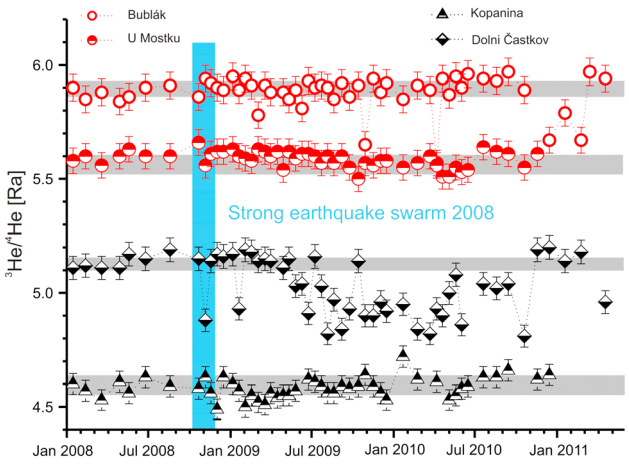

Figure 6. Time series of the $^3He/^4He$ ratios from two locations within the PPZ (Bublák and U Mostku) and two locations in the MLF (Dolni Častkov and Kopanina) in relation to 2008 swarm. The blue bar corresponds to the duration of the swarm. The gray bars correspond to the range of values in time of seismic quiescence [*after Bräuer et al.*, 2011], and the error bars represent 2σ.

The $\delta^{13}C$ values at the various monitored locations are interpreted to have been modified to varying degrees by CO_2-water interactions, as indicated by the variable gas/water ratios at the respective locations. A seasonal trend was also superimposed at the springs. This effect can be ignored at the gas-rich Bublák and Dolni Častkov mofettes (Figure 7). As a result repeated stronger changes were observed in the $\delta^{13}C$ values following the start of the seismically active period. A similar overall trend can be seen in the $\delta^{13}C$ values at both mofettes and also at Kopanina, associated with the 2008 swarm (Figure 7). The running average $\delta^{13}C$ value following the start of the swarm indicates a clear decrease in $\delta^{13}C$ values at the locations along the MLF, starting at Kopanina which is closest to the focal zone and occurring some time later at Dolni Častkov.

Different ^{15}N baseline signatures were determined for the five sampling locations on the basis of the monthly data recorded between May 2005 and June 2008 [*Bräuer et al.*, 2011]. There was greater variability in the $\delta^{15}N$ values from the start of the 2008 swarm than during periods of seismic quiescence, as was also observed for the monitored $\delta^{13}C$ values and $^3He/^4He$ ratios (Figure 8 and Table 1).

5. Discussion

Isotope-geochemical time series studies are a powerful tool for the evaluation of geodynamic processes. The NW Bohemia/Vogtland region is the only non-volcanic region in the world in which active geodynamic processes (earthquake swarms) have been the subject of detailed isotope time series studies [e.g., *Bräuer et al.*, 2003, 2008, 2011]. The only known comparably detailed isotope monitoring studies stemmed from investigations into volcanic activity in Italy [e.g., *Carapezza and Federico*, 2000; *Pecoraino and Giammanco*, 2005; *Capasso et al.*, 2005; *Rizzo et al.*, 2006; *Martelli et al.*, 2008; *Paonita et al.*, 2012].

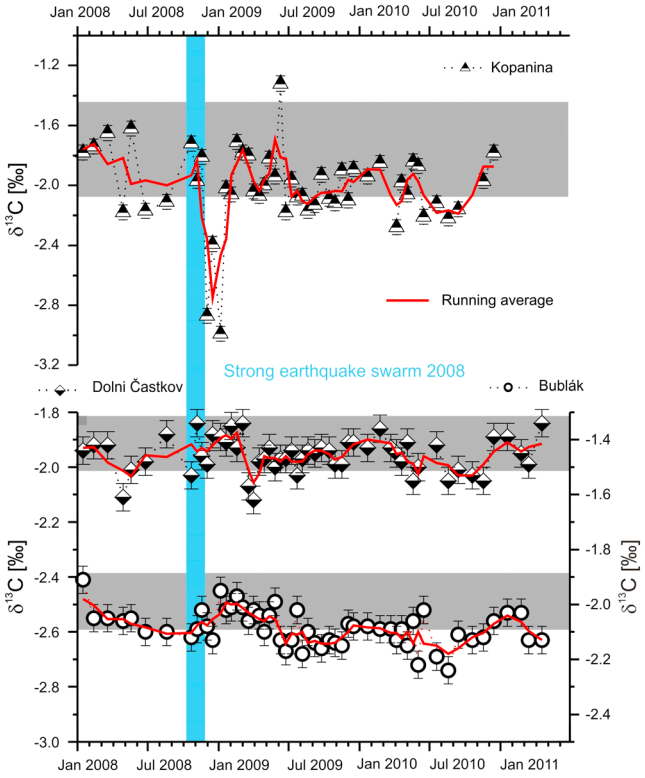

Figure 7. Time series of the $\delta^{13}C$ values from Bublák (PPZ), Dolni Častkov (MLF), and Kopanina (MLF) over a period covering 2008 earthquake swarm. The blue bar corresponds to the duration of the swarm. The gray bars correspond to the range of values in time of seismic quiescence [after *Bräuer et al.*, 2011], and the error bars represent 2σ. The red line corresponds to the running average of the $\delta^{13}C$ values.

The origin of the fluids in the investigation area and the seasonal effects, including CO_2-water interactions, at the monitored locations have previously been discussed in detail [e.g., *Bräuer et al.*, 2004, 2008, 2011]. The discussion of the latest time series data herein therefore focuses on new findings, in particular on the occurrence of fluid anomalies on two neighboring fault structures following the start of the 2008 swarm, on a comparison of the carbon and helium isotope patterns from the 2000 and 2008 earthquake swarms, and on the usefulness of detailed $\delta^{13}C$ studies for identifying magma degassing.

5.1. Temporal and Spatial Distribution of Anomalous Shifts of the Fluid Signatures Recorded at Locations Along the MLF and the PPZ Following the Start of the 2008 Swarm

Average values for the fluid characteristic during periods of seismic quiescence have previously been obtained from monthly data recorded between May 2005 and June 2008 [*Bräuer et al.*, 2011], providing an excellent basis for identifying seismically induced anomalies in the gas and isotope compositions along the two fault zones investigated (Figures 4–8). These data have also allowed the influence that seasonal variations have on the fluid signatures to be evaluated at the various monitoring locations [*Bräuer et al.*, 2011]. The gas/water ratio appears to be the dominant factor affecting the extent of seasonal influences on fluid signatures.

Figure 2 shows to the positions of the recorded seismic events ($M_L > 2$) in relation to the sampling locations, and to the MLF and PPZ. Isotope signatures modified by the seismically induced release of crust-derived components were repeatedly recorded at locations along the PPZ [e.g., *Bräuer et al.*, 2003, 2008, 2011] and at the Wettinquelle spring [*Bräuer et al.*, 2007]. Kopanina was the only location within the Nový Kostel epicentral area that was found to be releasing free gas, although the gas flow rate (~1 l/h) was very low compared to the Bublák site (~18,000 l/h). Gas and isotope compositions were, for the first time, monitored at locations along the MLF (at Kopanina and Dolni Častkov) from the start of a strong earthquake swarm.

The time series of $^3He/^4He$ ratios indicate stronger anomalies at the monitored locations along both the PPZ and the MLF, relative to the mean values from periods of seismic quiescence (Figure 6).

A clear decrease in the $^3He/^4He$ ratios was observed a few weeks before the start of the earthquake swarm in 2000 [*Bräuer et al.*, 2008]. This pre-seismic decrease in the $^3He/^4He$ ratios had been interpreted by strain changes of the rock associated with preparatory phase of the earthquake. However, no such anomalies could be identified for the October 2008 swarm because the monthly sampling terminated in June of that year; only minor variations in the $^3He/^4He$ ratios were observed before the start of this warm swarm. Repeatedly, a decrease of the $^3He/^4He$ isotope ratios was seen at all locations along the PPZ and the MLF over a period of at least 2 years following the start of the seismically active period (Figure 6 and Table 1). The anomalies occurred stronger at the mofettes than at the mineral springs, along both of the fault zones.

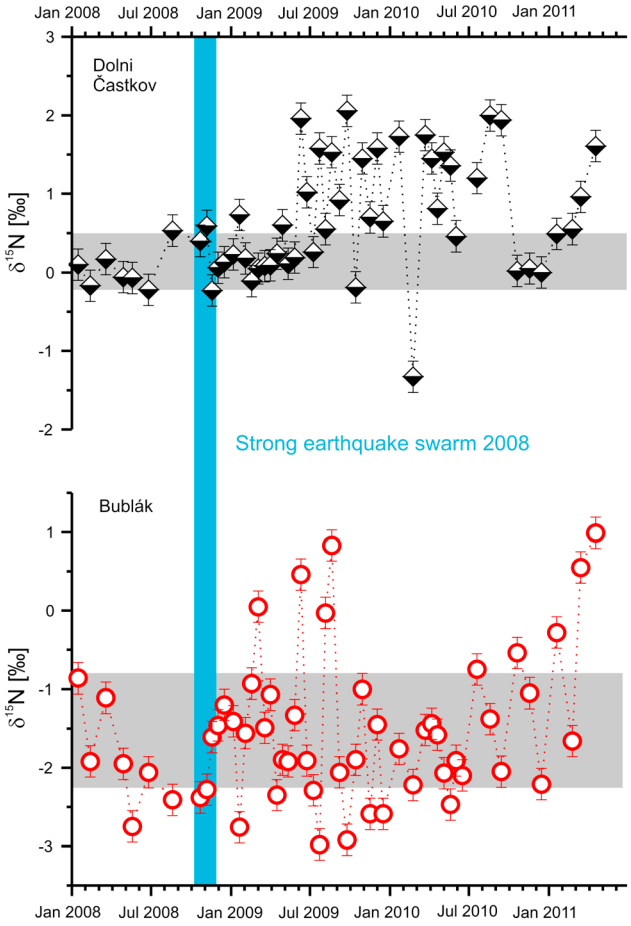

Figure 8. Time series of the $\delta^{15}N$ values from Bublák (PPZ) and Dolni Častkov (MLF) over a period covering 2008 earthquake swarm. The blue bar corresponds to the duration of the swarms. The gray bars correspond to the range of values in time of seismic quiescence [after *Bräuer et al.*, 2011], and the error bars represent 2σ.

The $^3He/^4He$ ratio is known to be a useful tool for distinguishing between crust and mantle-derived helium, with a decrease in $^3He/^4He$ ratios indicating the admixture of crust-derived helium. Surprisingly, distinctly larger variations in the $^3He/^4He$ ratios were detected along the MLF than along the PPZ, and the MLF thus seems to be more sensitive than the PPZ to the release of crust-derived components. This suggests that the focal zone may have been closer to the MLF than to the PPZ and/or that the migration pathways from the focal zone to the MLF were more permeable than the pathways to the PPZ.

As previously mentioned (subsection 4.1), the main component of the mantle-derived fluids at all monitoring locations was CO_2. The baseline isotope signature from CO_2 during periods of seismic quiescence was nearly the same for both the Bublák gas and the Dolni Častkov gas, which may be an indication that both locations are supplied from the same magmatic reservoir. The isotope signatures of helium and nitrogen indicate higher portions of crust-derived helium and nitrogen at the Dolni Častkov mofette [*Bräuer et al.*, 2011]. Minor mantle-derived components such as helium can only be transported from the magmatic reservoir to the surface by CO_2.

Different types of fluid transport processes need to be taken into account. The high $^3He/^4He$ ratios of the mantle-derived fluids suggest that their ascent must have taken place along highly permeable migration paths. Before seismically released crust-derived components can be transported with the mantle-derived fluid flow they need to migrate into the ascending channels. The rate of transport of crustal components released within the fractured zone is influenced by the different diffusion coefficients of the various gas components, which therefore enter the mantle-derived fluid flow at different times [*Torgersen and O'Donnell*, 1991].

The time series for the $\delta^{13}C$ values from Bublák, Dolni Častkov, and Kopanina are shown in Figure 7; the complete data set can be found in Table 1. The $\delta^{13}C$ time series from the Bublák and Dolni Častkov mofettes are shown as these gas-rich mofettes avoid the isotope fractionation effects that result from CO_2-water interactions, and the time series from Kopanina because this location is closest to the focal zone. The $\delta^{13}C$ patterns obtained from the PPZ (at Bublák) and the MLF (at Dolni Častkov) were similar to each other and also to the pattern obtained from the Kopanina data (Figure 7). Chemical and isotope fractionation effects dominate the $\delta^{13}C$ isotope pattern from U Mostku, and also the Wettinquelle data are superimposed by a seasonal trend [*Bräuer et al.*, 2011].

Changes in the $\delta^{13}C$ distribution patterns seem to start about 1 week after the start of the seismic swarm, occurring first on the MLF and then on the PPZ. In contrast to crust-derived helium, there is a broad range of $\delta^{13}C$ values in CO_2 that has been trapped or stored in crustal rocks. An upward migration of seismic activity during seismic swarms has been observed, with the earliest events occurring at the bottom of the activated

fault patch and subsequent events at progressively shallower depths (Figure 3). Fracturing may therefore occur in different rock units over time as a result of this migration of seismic events, and hence CO_2 with different $\delta^{13}C$ signatures may be released at different times. These crust-derived fluids migrate away from the hypocentral area: they can thus be admixed with the fluids flowing steadily from the upper mantle and hence transported to the earth's surface, where temporal modifications of isotope signatures from mantle-derived fluids have been repeatedly observed.

Following the start of the 2008 swarm, large fluctuations from the means were observed in the $\delta^{15}N$ values from both mofettes (Figure 8). Previous investigations into the gas from Bublák suggested a two-component mixture, with mantle-derived and atmosphere-derived components [*Bräuer et al*., 2004], whereas the $\delta^{15}N$ baseline signature values from Dolni Častkov suggest a three component mixture with different portions of mantle-, atmosphere-, and crust-derived nitrogen. The lower level of mantle-derived helium at Dolni Častkov than at Bublák, together with the higher helium concentration, fits well with the baseline ^{15}N signature at Dolni Častkov.

As with crust-derived CO_2 the additional admixture of crust-derived nitrogen must be associated with fracturing that occurred during the swarm. The seismically released crust-derived components must again have the opportunity to join the steady flow of mantle-derived fluid in order to verify temporally its isotope signature. Crustal reservoirs with different compositions may be successively opened as a result of the migration of the swarm's foci.

Mantle-derived nitrogen is generally depleted in ^{15}N [e.g., *Javoy and Pinot*, 1991; *Marty and Zimmermann*, 1999], while crust-derived nitrogen usually exhibits positive $\delta^{15}N$ values, with the degree of ^{15}N enrichment depending on the degree of metamorphism [e.g., *Haendel et al*., 1986; *Bebout and Fogel*, 1992; *Mingram and Bräuer*, 2001; *Sadofsky and Bebout*, 2004; *Cartigny and Marty*, 2013].

Those $\delta^{15}N$ values that are clearly higher than the "baseline" signature indicate a greater admixture of crust-derived nitrogen that continued until April 2011, when the monitoring was terminated. A number of different superimposed processes occurred during the earthquake swarm that may have affected the characteristics of mantle-derived fluid flow. The indications for the admixture of crust-derived nitrogen are stronger in the Dolni Častkov gas than in the Bublák gas, as was also suggested by the $^3He/^4He$ ratios.

5.2. Direct Comparisons of Seismically Triggered Fluid Anomalies Recorded During the Earthquake Swarms of 2000 and 2008

The range of hypocenter depths was almost the same for both the 2000 and 2008 swarms (6 to 11 km), but the maximum earthquake magnitudes (M_L 3.3 in 2000; M_L 3.8 in 2008) and the rates of energy release were different (Figure 3). The duration of the main swarm was about 10 weeks for the 2000 swarm and about 4 weeks for the 2008 swarm. Several phases could be distinguished within each of the swarms. Although an upward migration of the foci along the fault segment was noted for both swarms, a more detailed space-time distribution of the foci suggests a somewhat different pattern [*Fischer et al*., 2014].

A direct comparison of the isotope distribution patterns from the 2000 and 2008 earthquake swarms is only possible for the Wettinquelle spring, to the northwest of the Cheb Basin, and for the Bublák mofette within the PPZ. The records covering the earthquake swarm in 2000 commenced in May 2000, i.e., about 12 weeks before the start of the seismically active period.

At the Wettinquelle site we previously found a clear decrease in $^3He/^4He$ ratios (Figure 8b) immediately prior to the 2000 earthquake swarm. The helium isotope anomaly continued over a period about 6 weeks up to the start of the seismically active period, correlating with an anomaly in the groundwater level at a borehole in the Bad Brambach spa gardens, about 50 m from the Wettinquelle spring [*Koch et al*., 2003; *Bräuer et al*., 2007]. This anomaly has been interpreted as being related to strain changes within the country rock that occurred prior to fracturing, during the preparatory phase of the earthquake swarm. Such low level deformation may result in the mobilization of small molecules (such as He and H_2). In their review of hydrological and geochemical studies directed toward earthquake prediction, *Matsumoto and Koizumi* [2013] evaluated geochemical precursor anomalies and concluded that increases in gas release were commonly observed prior to seismicity but that details of the mechanisms involved in the temporal occurrence of the geochemical anomalies recorded at the earth's surface remain unclear. As mentioned above, no such pre-seismic signal was detected prior to the 2008 swarm. However, the release of small molecules cannot be ruled

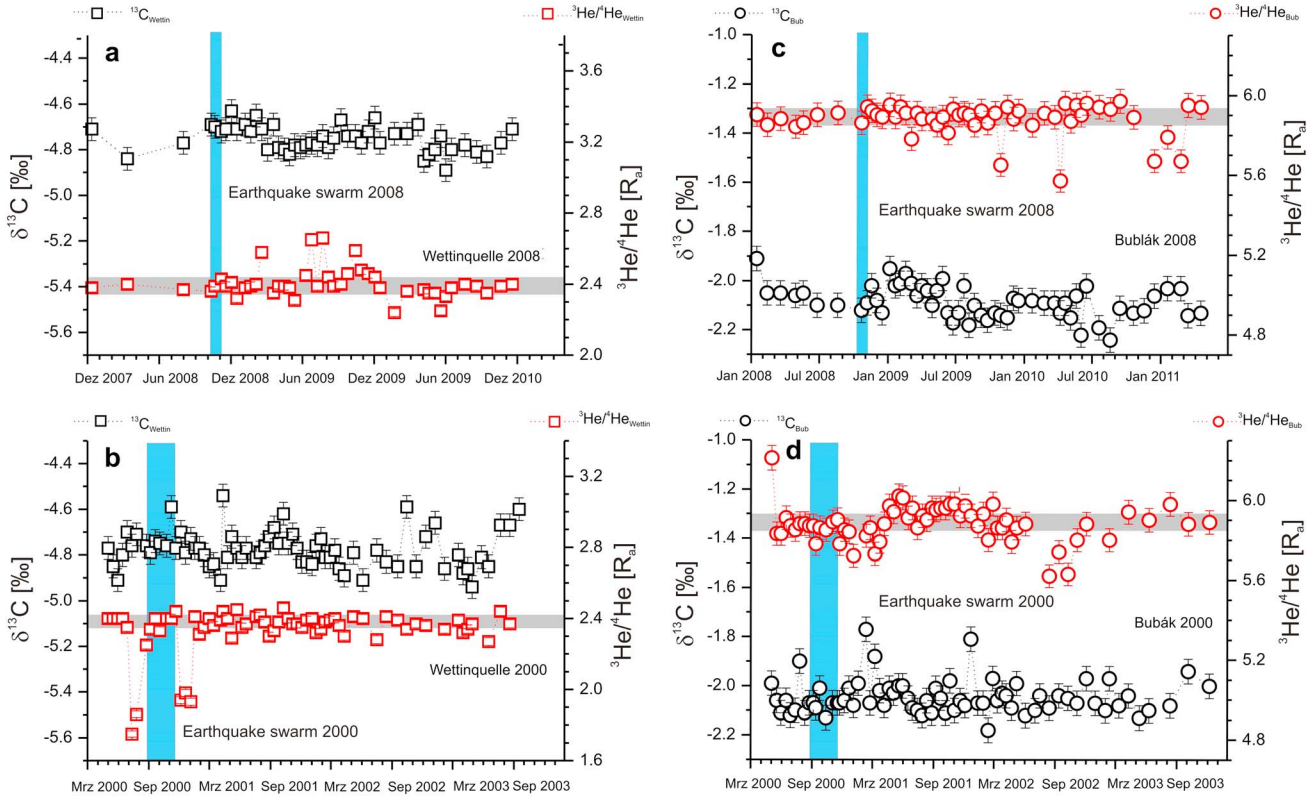

Figure 9. Time series of the $\delta^{13}C$ values (black squares) and the $^3He/^4He$ ratios (red squares) from Wettinquelle covering the seismically active periods in 2008 (a) and 2000 (b), together with time series data from the Bublák mofette in 2008 (c) and 2000 (d) ($\delta^{13}C$ = black circles; $^3He/^4He$ = red circles). At the Wettinquelle spring the deviation in the measured $^3He/^4He$ ratios was smaller than the symbols. The gray bars represent the range of $^3He/^4He$ ratios during times of seismic quiescence [*Bräuer et al.*, 2011]. The blue bars represent the durations of the swarms. The 2000 data can be found in *Bräuer et al.* [2007, 2008]. During the fluid monitoring in 2000, the $\delta^{13}C$ values were recorded weekly and the $^3He/^4He$ ratios every 2 weeks [*Bräuer et al.*, 2008]. For better comparability Figures 8b and 8d show only data from samples in which both $\delta^{13}C$ values and $^3He/^4He$ ratios were analyzed.

out because the last sampling prior to the 2008 swarm was carried out in June 2008 and was therefore not suitable for the detection of any such anomalies.

Both differences and similarities have been noted between the helium isotope patterns for the 2000 and 2008 swarms from the Wettinquelle spring (Figures 9a and 9b). From the start of the seismically active periods in both 2000 and 2008, the $^3He/^4He$ ratios repeatedly decreased compared with the mean values for periods of seismic quiescence, suggesting the admixture of crust-derived helium. However, following the start of the 2008 swarm several distinct increases in the $^3He/^4He$ ratios were recorded from the Wettinquelle gas (Figure 9a). The mean value of the $^3He/^4He$ ratios during periods of seismic quiescence was 2.38 ± 0.04 Ra [*Bräuer et al.*, 2011].

Distinct increases in the $^3He/^4He$ ratios were recorded in 2006 at monitoring locations along the PPZ, while the $^3He/^4He$ ratios from the Wettinquelle spring remained at average levels [*Bräuer et al.*, 2011]. *Bräuer et al.* [2009] interpreted the increased $^3He/^4He$ ratios from the monitoring locations in the Cheb Basin as indicating the supply of fresh magma from a less degassed, deeper reservoir and inferred that the earthquake swarm in 2008 may have been triggered by this hidden magmatic process. A time delay between gas anomalies and seismic events is not unusual. A delay of several months was, for example, observed by *Martens and White* [2013] between the ascent of magma in Iceland's Northern Volcanic Rift Zone and the seismicity triggered by this event. *Martens and White* [2013] suggested that carbon dioxide exsolved at far greater depths than the dyke intrusion may have triggered the seismicity. Detailed investigations into seismic activity at Mammoth Mountains in eastern California found low Vp/Vs ratios within the upwardly migrating seismicity, suggesting the involvement of fluid (CO_2) in the seismic swarm [*Lin*, 2013]. Progressively increasing Vp/Vs ratios were recorded before the April 2006 L'Aquila earthquake in Italy. The increased Vp/Vs ratios were probably based

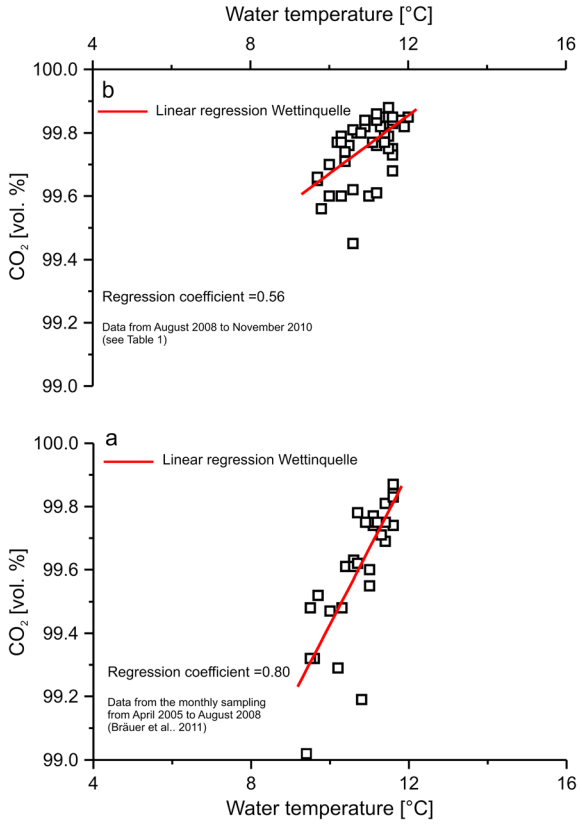

Figure 10. Linear fit between water temperature and CO_2 of the time series at the Wettinquelle accompanying the 2008 swarm compared with data from times of seismic quiescence [from *Bräuer et al.*, 2011].

on an increment of pore fluid pressure, and the spatial anisotropy of Vp/Vs ratios suggests the movement of fluids along the fault planes. *Di Luccio et al.* [2010] concluded that deep fluids were more likely to have controlled the process than tectonic stress. That migrating fluids can bring a fault system to a critical state was indicated when wastewater was injected in the mid-western United States, resulting in a clear increase in seismicity recorded between 6 and 20 months after the injection [*van der Elst et al.*, 2013].

The repeated increases in $^3He/^4He$ ratios recorded from the Wettinquelle spring between 2008 and 2010 (Figure 9a) may also have been the result of the indicated ongoing hidden magmatic process beneath the Cheb Basin [*Bräuer et al.*, 2009]. A distinct increase in the $^3He/^4He$ ratio was recorded from the Bublák mofette in May 2000 (Figure 9d), at the start of the monitoring period, possibly also reflecting a supply of fresh magma prior to the swarm of 2000.

Decreased $^3He/^4He$ ratios were repeatedly observed at the Bublák mofette after the 2008 swarm, confirming the admixture of seismically induced crust-derived helium (Figure 9c).

The interpretation of the $\delta^{13}C$ values is less clear than for the $^3He/^4He$ ratios because, in contrast to helium, CO_2 reacts with water. At the Bublák mofette the gas escapes from a small pool of CO_2 saturated surface water (pH ~4.4; conductivity ~100 μS/cm). The influence of temperature-dependent isotope fractionation can be neglected here, but the gas flow at the Wettinquelle spring was clearly less than the water discharge and the pH and conductivity values were clearly higher, resulting in the formation of bicarbonate. Temperature-dependent isotope fractionation therefore needs to be taken into account at the Wettinquelle; the fractionation effect has been previously discussed in detail in *Bräuer et al.* [2007, 2008]. This temperature dependency has produced a seasonal trend in the $\delta^{13}C$ values at the Wettinquelle spring. During periods of seismic quiescence the CO_2 concentration at the Wettinquelle spring correlated with the water temperature (Figure 10a). This correlation was, however, interrupted following the start of the 2008 earthquake swarm (Figure 10b). A similar deviation from the seasonal trend was previously observed at the Wettinquelle spring accompanying the 2000 earthquake swarm [*Bräuer et al.*, 2007].

The Wettinquelle spring is supplied by a mixture of water with a tritium content of approximately 4TU and an older tritium-free, more highly mineralized water component. The spring water at Wettinquelle exhibits a hydrochemical sensitivity to pressure fluctuations within the aquifer that result in short-term variations in the mixing ratios of these two water types during hydrologically extreme periods [*Koch et al.*, 2005]. Such short-term increases in the admixture of less mineralized water could also have influenced the $\delta^{13}C$ values.

Figure 11 shows the measured $\delta^{13}C$ values, together with the water temperatures. From July 2009 to October 2010 the $\delta^{13}C$ values deviated repeatedly from the seasonal trend (Figure 11a). Deviations of the $\delta^{13}C$ values from the seasonal trend were also observed following the start of the 2000 swarm, between 2001 and November 2003 (Figure 11b). It was assumed that CO_2 released by fracturing within the focal zone was temporarily admixed with the mantle-derived fluid flow [*Bräuer et al.*, 2008]. Previous studies have indicated that the degassing locations to the north of the Cheb Basin were supplied with mantle-derived fluids from the same magmatic reservoir as the degassing location along the PPZ and MLF [*Bräuer et al.*, 2004, 2008].

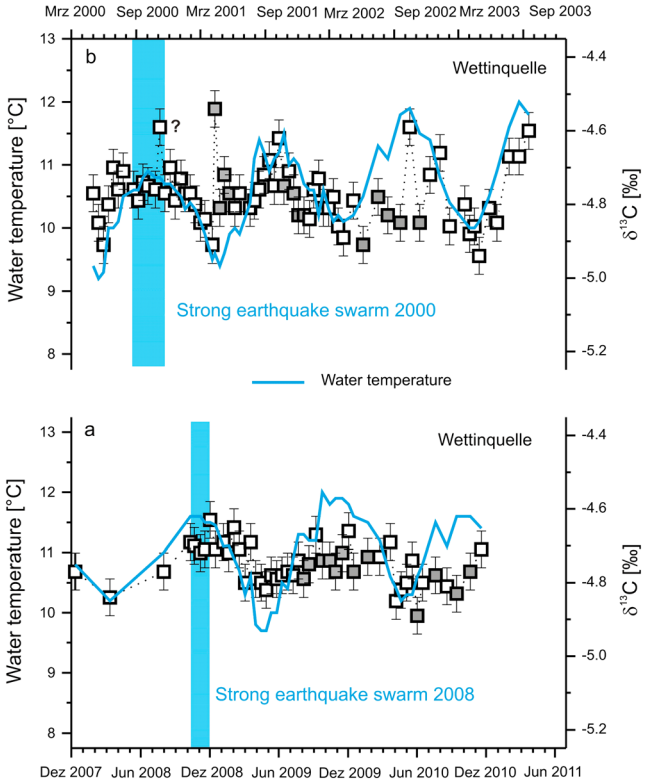

Figure 11. Measured $\delta^{13}C$ values from the Wettinquelle spring over a period covering the swarms of 2000 and 2008 are shown together with the water temperatures. The blue bars indicate the duration of the swarms. The filled quarters point to $\delta^{13}C$ values deviated from the seasonal trend. Data for the 2000 swarm are from *Bräuer et al.* [2007].

Seismically released crust-derived components may occur in the Wettinquelle gas some time after the swarm started.

Apart from carbonate rocks most of the CO_2 in the crust is trapped in fluid inclusions and is therefore likely to be released by fracturing. In contrast, helium is produced steadily within the earth's crust and admixed with mantle-derived fluids along their migration pathways. The CO_2 trapped in fluid inclusions exhibits a wide range of $\delta^{13}C$ values, and different crustal reservoirs may be opened due to the migration of the hypocenters (Figure 3). Studies of $\delta^{13}C_{CO2}$ values from CO_2-dominated inclusions of metamorphic and granitic units are scarce, and no such data are known from the western Eger Rift area. Carbon isotopic data have, however, been reported by *Reutel* [1992] from the vicinity of the KTB, approximately 50 km southwest of the monitoring locations in the Cheb Basin. Fluid inclusions in quartz with different degrees of metamorphism, and also in granites, were investigated, with $\delta^{13}C$ values ranging from -4 to -18‰. The CO_2 from inclusions in the granitic units tends to be more enriched in $\delta^{13}C$, with values reaching up to -4‰ in the vicinity of the KTB. More recent inclusion studies on samples from metamorphic quartz veins in the Attic Cycladic Massif (Greece) yielded $\delta^{13}C$ values that ranged from -2.5 to -0.9‰ [*Siebenaller et al.*, 2013]. The $\delta^{13}C$ values at the degassing locations may therefore be temporarily increased or decreased as a result of the admixture of released CO_2 from different rock units.

According to *Fischer et al.* [2010] the foci of the 2008 earthquake swarm lay on precisely the same fault section in the Nový Kostel focal zone as was activated by the 2000 swarm ($M_L \leq 3.2$); the steeply dipping fault planes appear to be identical, taking into account the location error of about 100 m. A later, more detailed study of the space-time distribution of the foci, however, showed a different pattern, with a counter-clockwise migration in the 2000 swarm and a gradual upward migration in the 2008 swarm [*Fischer et al.*, 2014].

Changes in the characteristics of seismohydrological anomalies associated with the earthquake swarms of 2000 and 2008 were also observed. The main distinguishing features between both swarms lie in their hydraulic pressure anomalies, with differences having been noted in the number of anomalies as well as in their shapes and the durations), which may possibly relate to the different migration behavior of the foci over time [*Koch and Heinicke*, 2011].

The observed differences in the behavior of the foci during the swarms may have influenced the migration of the released crust-derived fluids. Differences in the isotope patterns of the helium and CO_2 components, which are mainly mantle derived, were observed at the Wettinquelle and Bublák locations following the start of the 2000 and 2008 swarms, respectively (Figure 9). Features that the two swarms had in common were the evidence for seismically induced release of crust-derived helium and anomalous $\delta^{13}C$ values that occurred mainly after the start of the seismically active period.

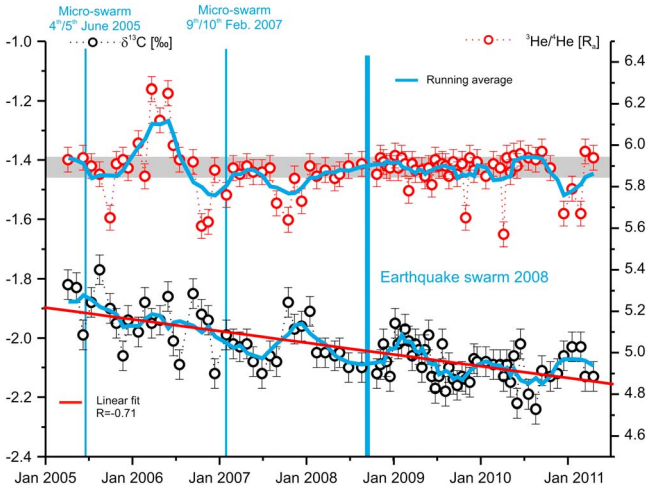

Figure 12. Time series of $^3He/^4He$ ratios and $\delta^{13}C$ means from each pair of samples collected from the Bublák mofette between 2005 and 2011. The blue bars indicate the duration of the swarms. The gray bar represents the range of $^3He/^4He$ ratios during times of seismic quiescence [*Bräuer et al.*, 2011]. The blue curves correspond to the running average, and the red line represents the linear fit of the $\delta^{13}C$ values.

In summary, comparing the recorded isotope data from the 2000 and 2008 swarms shows evidence for the superimposition of seismically and magmatically driven processes.

5.3. Evidence of Magma Degassing From a Detailed Carbon Isotope Time Series (Bublák, 2005–2011)

As mentioned above, $^3He/^4He$ ratios are the best tool available for distinguishing between crust- and mantle-derived fluids. The $^3He/^4He$ ratios in the free gas phase from the Bublák mofette have been monitored since 2000. As a result clear evidence of ongoing hidden magmatic processes has been found at locations in the eastern part of the Cheb Basin [*Bräuer et al.*, 2005], which has since been confirmed by more recent data (*Bräuer et al.*, 2009, 2011]. The increase in mantle-derived helium correlates with an increase in gas flow, indicating that the Bublák mofette field is a deep-reaching fluid injection zone [*Kämpf et al.*, 2013]. Investigations at the Mount Etna volcano over the last 20 years have repeatedly noted an increase in soil CO_2 flux before eruptions, and correlations between ascending magma and the occurrence of seismicity have been confirmed by complex studies indicating the interplay of a number of different processes [*Federico et al.*, 2011]. In contrast to the Mount Etna situation where the transport of magma occurs mainly at shallow depths within the crust, *Bräuer et al.* [2008] inferred magmatic reservoirs at different depths within the lithospheric mantle beneath NW Bohemia. The supply of fresh, less degassed, magma from such subcontinental lithospheric reservoirs may be indicated by $^3He/^4He$ ratios >6 Ra, as were found before the earthquake swarm of 2000, and also in the spring of 2006 prior to the strong earthquake swarm in 2008 [*Bräuer et al.*, 2009]. The Bublák gas therefore seems to likely have the greatest geodynamic significance for the evaluation of ongoing geodynamic processes in the Eger Rift.

CO_2 is known to be the main magmatic component of escaping mantle-derived fluids in non-volcanic regions. We therefore carried out detailed investigations into the $\delta^{13}C$ values from Bublák, for which we collected duplicate samples between May 2005 and April 2011. The difference between the $\delta^{13}C$ values obtained from each pair of samples was generally <0.05‰. Chemical and isotope fractionation effects due to CO_2-water interactions can be neglected at the Bublák mofette because of the high gas flow, and also because the water pool through which the gas escapes is always CO_2 saturated and has a low pH (~4.4). This means that the observed variations in $\delta^{13}C$ values (Figure 12) reflect the characteristics of both the progressively degassing magma and the effect of CO_2 that has been released by fracturing from crustal rocks and admixed with the mantle fluid flow during migration through the lithosphere. The state of magma degassing affects the $\delta^{13}C$ values of the released gas: the gas released from basaltic melts has been found to be enriched by about 2‰ relative to the parent melt [*Mattey*, 1991]. The highest $\delta^{13}C$ values should therefore occur at the beginning of the degassing and should then decrease progressively over time. The $\delta^{13}C$ values of the gas should decrease continually following the supply of less degassed magma from a deeper reservoir to a reservoir in the uppermost mantle [*Bräuer et al.*, 2011]. However, the degassing effects of two interacting magma reservoirs at different depths within the upper mantle are superimposed by the seismic release of CO_2 trapped in the crust. This seismically released CO_2 migrates away from the focal zone and may be admixed with the steady flow of mantle-derived fluids, complicating the $\delta^{13}C$ pattern and rendering its interpretation more difficult. Nonetheless, the linear fit of the $\delta^{13}C$ values between 2005 and 2011 indicates decreasing $\delta^{13}C$ values over time (Figure 12). Provided the first step of the crustal released fluid transport after fracturing depends on the different diffusion coefficients of the gas components, the simultaneous

occurrence of isotope anomalies cannot be expected. Following the period of increased $^3He/^4He$ ratios in spring 2006, repeated periods with lower $^3He/^4He$ ratios appear to correlate with increased $\delta^{13}C$ values (see Figure 12 for running averages). The inverse trend was observed independent from the overall decreasing trend of the $\delta^{13}C$ values during the complete monitoring period. Magma degassing appears to have a greater effect on $\delta^{13}C$ values than on helium isotope ratios, possibly because of the greater differences in solubility between CO_2 and helium within the melt than between ^3He and ^4He. Repeatedly decreased $^3He/^4He$ ratios occurred during the monitoring period indicating the admixture of crust-derived helium of seismically triggered release of crust-derived helium whose release had been seismically triggered (Figure 12). The situation is further complicated by the possibility that different forms of carbon (CO_2; CO_3^{2-}) may coexist within the melt. The carbon fractionation effect may then also depend on the mixing ratio of the two components within the melt [e.g., *Paonita et al*., 2013 and references therein].

It is important to remember that the data were only recorded every 2 weeks, and hence not all seismically triggered geochemical anomalies have necessarily been identified.

Data from isotope-geochemical monitoring are being increasingly used for the evaluation of ongoing geodynamic processes, and our latest results confirm the benefit of such data for this purpose. There have been few comparable detailed geochemical studies carried out to date, and since any other monitoring has been carried out in the vicinity of active volcanoes, e.g., within the Mount Etna degassing system [*Paonita et al*., 2012 and references therein], they unfortunately have only limited comparability with our investigations. Nevertheless, similar isotope distribution patterns are known from Mount Etna degassing volatiles, indicating both seismically triggered release and magma movement.

Conclusions

1. The anomalies recorded in relation to the 2008 earthquake swarm match well with the results from investigations into the 2000 swarm [*Bräuer et al*., 2008]. Anomalies in the isotope composition ($^3He/^4He$; $\delta^{13}C$; $\delta^{15}N$) were observed to continue for at least 2 years after the commencement of increased seismic activity in both events, suggesting similar fluid migration behavior.
2. In order to identify geodynamically triggered anomalies in fluid signatures it is important to take into account both hydrological and seasonal variations. Gas-rich mofettes appear to be better suited for tracing seismically induced and/or magma-driven processes because hydrological and seasonal variations are negligible at these locations.
3. Differences in the detailed seismic character of the 2008 earthquake swarm correlate with modifications to the isotope distribution patterns recorded between 2008 and 2011.
4. Anomalies in the fluid signatures were observed from the start of the 2008 earthquake swarm at locations along both the PPZ and the MLF. There were differences in the temporal and spatial distributions of these anomalies, as well in their strengths, probably due to the position of the respective fault zone relative to the Nový Kostel focal zone and/or to variations in the permeability of the migration pathways followed by the steady flow of mantle-derived fluids.
5. The pre-seismic increases in $^3He/^4He$ ratios recorded from the Bublák mofette suggest that both the 2000 and 2008 swarms were associated with ongoing hidden magmatic processes in the lithospheric mantle, beneath the epicentral area.
6. The distribution pattern for $\delta^{13}C$ obtained from detailed studies at Bublák between 2005 and 2011 has, for the first time, identified a hidden, progressive, magma degassing process. The effects of ongoing magma degassing are superimposed on seismically induced variations in the $\delta^{13}C$ signature.
7. Detailed monitoring of the isotope composition of degassing volatiles is an excellent tool for evaluation of the geodynamic situation within a region, and is ideally suited to tracing fluid migration and variations in fluid sources.

Acknowledgments
The authors would like to thank J. Sültenfuß (University of Bremen, Institute of Environmental Physics) for the $^3He/^4He$ ratio measurements and J. Tesař (Laborunion CZ, Františkový Lázně) for the gas composition measurements. Technical assistance was provided by W. Städter. The authors would also like to thank WC Evans and an anonymous reviewer for their helpful comments and their appreciation of this work. The project was kindly funded by the German Science Foundation (BR 1396/5, STR 376/11, KA 902/16).

References

Babuška, V., J. Plomerová, and T. Fischer (2007), Intraplate seismicity in the western Bohemian Massif (central Europe): A possible correlation with a paleoplate junction, *J. Geodyn.*, *44*, 149–159.

Bankwitz, P., G. Schneider, H. Kämpf, and E. Bankwitz (2003), Structural characteristics of epicentral areas in central Europe: Study case Cheb Basin (Czech Republic), *J. Geodyn.*, *35*, 5–32.

Bebout, G. E., and M. L. Fogel (1992), Nitrogen-isotope composition of metasedimentary rocks in the Catalina Schist, California: Implications for metamorphic devolatilization history, *Geochim. Cosmochim. Acta*, *56*, 2839–2849.

Bräuer, K., H. Kämpf, G. Strauch, and S. M. Weise (2003), Isotopic evidence ($^3He/^4He$, $^{13}C_{CO2}$) of fluid triggered intraplate seismicity, *J. Geophys. Res.*, *108*(B2), 2070, doi:10.1029/2002JB002077.

Bräuer, K., H. Kämpf, S. Niedermann, G. Strauch, and S. M. Weise (2004), Evidence for a nitrogen flux directly derived from the European subcontinental mantle in the Western Eger Rift, central Europe, *Geochim. Cosmochim. Acta*, *68*, 4935–4937.

Bräuer, K., H. Kämpf, S. Niedermann, and G. Strauch (2005), Evidence for ascending upper mantle-derived melt beneath the Cheb Basin, central Europe, *Geophys. Res. Lett. 32*, L08303, doi:10.1029/2004GL022205.

Bräuer, K., H. Kämpf, U. Koch, S. Niedermann, and G. Strauch (2007), Seismically induced changes of the fluid signature detected by a multi-isotope approach (He, CO2, CH4, N2) at the Wettinquelle, Bad Brambach (central Europe), *J. Geophys. Res.*, *112*, B04307, doi:10.1029/2006JB004404.

Bräuer, K., H. Kämpf, S. Niedermann, G. Strauch, and J. Tesař (2008), The natural laboratory NW Bohemia – Comprehensive fluid studies between 1992 and 2005 used to trace geodynamic processes, *Geochem. Geophys. Geosyst.*, *9*, Q04018, doi:10.1029/2007GC001921.

Bräuer, K., H. Kämpf, and G. Strauch (2009), Earthquake swarms in non-volcanic regions: What fluids have to say, *Geophys. Res. Lett. 36*, L17309, doi:10.1029/2009GL039615.

Bräuer, K., H. Kämpf, U. Koch, and G. Strauch (2011), Monthly monitoring of gas and isotope compositions in the free gas phase at degassing locations close to the Nový Kostel focal zone in the western Eger Rift, Czech Republic, *Chem. Geol.*, *290*, 163–176.

Capasso, G., M. L. Carapezza, C. Federico, S. Inguaggiato, and A. Rizzo (2005), Geochemical monitoring of the 2002-2003 eruption at Stromboli volcano (Italy): Precurory changes in the carbon and helium isotopic composition of fumarole gases and thermal waters, *Bull. Volcanol.*, *68*, 118–134.

Caracausi, A., F. Italiano, G. Martinelli, A. Paonita, and A. Rizzo (2005), Long-term geochemical monitoring and extensive/compressive phenomena: Case study of the Umbria Region (Central Apennines, Italy), *Ann. Geophys.*, *48*, 43–53.

Carapezza, M. L., and C. Federico (2000), The contribution of fluid geochemistry to the volcano monitoring of Stromboli, *J. Volcanol. Geotherm. Res.*, *95*, 227–245.

Cartigny, P., and B. Marty (2013), Nitrogen isotopes and mantle geodynamics: The emergence of life and atmosphere-crust-mantle connection, *Elements*, *9*, 359–366.

Chiodini, G., A. Caliro, C. Cardellini, C. F. Frondini, S. Inguaggiato, and F. Matteucci (2011), Geochemical evidence for and charaterization of CO2 rich gas sources in the epicentral area of the Abruzzo 2009 earthquakes, *Earth Planet. Sci. Lett.*, *304*, 389–398.

Credner, H. (1876), Das vogtländisch-erzebirgische Erdbeben vom 23. November 1875, *Z. Ges. Naturwiss.*, *48*, 246–269.

Di Luccio, F., G. Ventura, R. Di Giovambattista, A. Piscini, and F. R. Cinti (2010), Normal faults and thrusts reactivated by deep fluids: The 6 April 2009 Mw 6.3 L'Aquila earthquake, central Italy, *J. Geophys. Res.*, *115*, B06315, doi:10.1029/2009JB007190.

Federico, C., M. Camarda, S. De Gregorio, and S. Gurrieri (2011), Long-term record of CO_2 degassing along Mt. Etna's flanks and its relationship with magma dynamics and eastern flank instability, *Geochem. Geophys. Geosyst.*, *12*, Q10002, doi:10.1029/2011GC003601.

Fischer, T., J. Horálek, J. Michálek, and A. Bouškova (2010), The 2008 West Bohemia earthquake swarm in the light of the WEBNET network, *J. Seismol.*, *14*, 665–682.

Fischer, T., J. Horálek, P. Hrubcová, V. Vavryčuk, K. Bräuer, and H. Kämpf (2014), Intra-continental earthquake swarms in west-Bohemia and Vogtland: A review, *Tectonophysics*, *611*, 1–27.

Gautheron, C., M. Moreira, and C. Allègre (2005), He, Ne and Ar composition of the European lithospheric mantle, *Chem. Geol.*, *217*, 97–112.

Geissler, W. H., H. Kämpf, R. Kind, K. Bräuer, K. Klinge, T. Plenefisch, J. Horálek, J. Zednik, and V. Nehybka (2005), Seismic structure and location of a CO_2 source in the upper mantle of the western Eger (Ohře) Rift, central Europe, *Tectonics*, *24*, TC5001, doi:10.1029/2004TC001672.

Gold, T., and S. Soter (1984), Fluid ascent through the solid lithosphere and its relation to earthquakes, *Pure Appl. Geophys.*, *122*, 492–530.

Gulec, N., D. R. Hilton, and H. Mutlu (2002), Helium isotope variations in turkey: Relationship to tectonics, volcanism and recent seismic activities, *Chem. Geol.*, *187*, 129–142.

Haendel, D., K. Mühle, H.-M. Nitzsche, G. Stiehl, and U. Wand (1986), Isotopic variations of fixed nitrogen in metamorphic rocks, *Geochim. Cosmochim. Acta*, *50*, 749–758.

Hainzl, S., T. Fischer, and T. Dahm (2012), Seismicity-based estimation of the driving fluid pressure in case of swarm activity in Western Bohemia, *Geophys. J. Int.*, *191*, 271–281.

Heuer, B., W. H. Geissler, R. Kind, and H. Kämpf (2006), Seismic evidence for asthenospheric updoming beneath the western Bohemian Massif, central Europe, *Geophys. Res. Lett.*, *33*, L05311, doi:10.1029/2005GL025158.

Heuer, B., W. H. Geissler, R. Kind, and the BOHEMA working group (2011), Receiver function search for a baby plume in the mantle transition zone beneath the Bohemian Massif, *Geophys. J. Int.*, *187*, 577–594.

Hill, D. P. (1977), A model for earthquake swarms, *J. Geophys. Res.*, *82*, 1347–1352, doi:10.1029/JB082i008p01347.

Hilton, D. L. (1996), The helium and carbon isotope systematics of a continental geothermal system: Results from monitoring studies at Long Valley caldera (California, U.S.A.), *Chem. Geol.*, *127*, 269–295.

Horálek, J., A. Bouśková, F. Hampl, and T. Fischer (1996), Seismic regime of the West-Bohemian earthquake swarm region: Preminінary results, *Stud. Geophys. Geod.*, *40*, 398–412.

Horálek, J., T. Fischer, A. Bouškova, J. Michálek, and P. Hrubcová (2009), The West Bohemia 2008-Earthquake swarm: When, where, what size and data, Stud, *Geophys. Geod.*, *53*, 351–358.

Hrubcová, P., and W. H. Geissler (2009), The Crust-Mantle Transition and the Moho beneath the Vogtland/West Bohemian Region in the Light of Different Seismic Methods, *Stud. Geophys. Geod.*, *53*, 275–294.

Hrubcová, P., V. Vavryčuk, A. Bouśková, and J. Horálek (2013), Moho depth determination from waveforms of microearthquakes in the West Bohemia/Vogtland swarm area, *J. Geophys. Res. Solid Earth*, *118*, 1–17, doi:10.1029/2012JB009360.

Ibs-von Seht, M., T. Plenefisch, and K. Klinge (2008), Earthquake swarms in continental rifts – A comparison of selected cases in America, Africa and Europe, *Tectonophysics*, *452*, 66–77.

Irwin, W. P., and I. Barnes (1980), Tectonic relations of carbon dioxide discharges and earthquakes, *J. Geophys. Res.*, *85*, 3115–3121, doi:10.1029/JB085iB06p03115.

Javoy, M., and F. Pinot (1991), The volatiles record of a "popping" from Mid-Atlantic Ridge at 14°N: Chemical and isotope composition of trapped gas in vesicles, *Earth Planet. Sci. Lett.*, *107*, 598–611.

Kämpf, H., K. Bräuer, J. Schumann, K. Hahne, and G. Strauch (2013), CO_2 discharge in an active, non-volcanic continental rift area (Czech Republic): Characterisation ($\delta^{13}C$, $^3He/^4He$) and quantification of diffuse and vent CO_2 emissions, *Chem. Geol.*, *339*, 71–83.

Knett, J. (1899), Das Erzgebirgische Swarmbeben zu Hartenberg vom 1 Jänner bis Feber 1824, *Sitzungsber. Deutsch. Naturwiss. — med Ver. Böhmen, Lotos Prag N.F.*, *19*, 167–191.

Koch, U., J. Heinicke, and M. Voßberg (2003), Hydrogeological effects of the latest Vogtland-NW Bohemian swarmquake period (August to December 2000), *J. Geodyn.*, *35*, 107–123.
Koch, U., D. Herbert, M. Voßberg, and J. Henicke (2005), Auswirkungen der Fassungssanierung der Wettinquelle Bad Brambach, auf die Altersstruktur des Mineralwassers, *Grundwasser*, *2*, 102–113.
Koch, U., and J. Heinicke (2011), Seismohydrological effects related to the NW Bohemia earthquake swarms of 2000 and 2008: Similarities and distinctions, *J. Geodyn.*, *51*, 44–52.
Lin, G. (2013), Seismic investigation of magmatic unrest beneath Mammoth Mountains California, USA, *Geology*, *41*, 847–850.
Martelli, M., A. Caracausi, A. Paonita, and A. Rizzo (2008), Geochemical variations of air-free crater fumeroles at Mt. Etna: New inferences for forecasting shallow volcanic activity, *Geophys. Res. Lett.*, *35*, L21302, doi:10.1029/2008GL035118.
Martens, H. R., and R. S. White (2013), Triggering of microearthquakes in Iceland by volatiles released from a dyke intrusion, *Geophys. J. Int.*, *194*, 1738–1754.
Marty, B., and L. Zimmermann (1999), Volatiles (He, C, N, Ar) in mid-ocean ridge basalts: Assessment of shallow-level fractionation and characterization of source composition, *Geochim. Cosmochim. Acta*, *63*, 3619–3633.
Mattey, D. P. (1991), Carbon-dioxide solubility and carbon isotope fractionation in basaltic melt, *Geochim. Cosmochim. Acta*, *55*, 3467–3473.
Matsumoto, N., and N. Koizumi (2013), Recent hydrological and geochemical research for earthquake prediction in Japan, *Nat. Hazards*, *69*, 1247–1260.
Mingram, B., and K. Bräuer (2001), Ammonium concentration and nitrogen isotope composition in metasedimentary rocks from different tectonometamorphic units of the European Variscan Belt, *Geochim. Cosmochim. Acta*, *65*, 273–287.
Mrlina, J., H. Kämpf, C. Kroner, J. Mingram, M. Stebich, A. Brauer, W. H. Geissler, J. Kallmeyer, H. Matthes, and M. Seidl (2009), Discovery of the first Quaternary maar in the Bohemian Massif, Central Europe, based on combined geophysical and geological surveys, *J. Volcanol. Geotherm. Res.*, *182*, 97–112.
Paonita, A., A. Caracausi, G. Iacono-Marziano, M. Martelli, and A. Rizzo (2012), Geochemical evidence for mixing between fluids exsolved at different depths in the magmatic system of Mt Etna (Italy), *Geochim. Cosmochim. Acta*, *84*, 380–394.
Paonita, A., C. Federico, P. Bonfanti, G. Capasso, S. Inguaggiato, F. Italiano, P. Madonia, G. Pecoraino, and F. Sortino (2013), The episodic and abrupt geochemical changes at La Fossa fumaroles (Vulcano Island, Italy) and related constrains on the dynamics, structure, and compositions of the magmatic system, *Geochim. Cosmochim. Acta*, *120*, 158–178.
Pecoraino, G., and S. Giammanco (2005), Geochemical characterization and temporal changes in parietal gas emissions at Mt. Etna (Italy) during the period July 2000-July 2003, *TAO*, *16*, 805–841.
Proft, E. (1894), Kammerbühl und Eisenbühl, die Schichtvulkane des Egerer Beckens, *Jahrb. Geol. Reichsanstalt Wien*, *44*, 25–85.
Reutel, C. (1992), Krustenfluide in Gesteinen und Lagerstätten am Westrand der Böhmischen Masse, *Göttinger Arb. Geol. Paläontol.*, 53, Geol. Inst., Univ. Göttingen, Göttingen, Germany.
Rizzo, A. R. R. Caracausi M. Favara A. Martelli M. Paonita P. M. N. Paternoster, and A. Rosciglione (2006), New insights into magma dynamics during last two eruptions of Mount Etna as inferred by geochemical monitoring from 2002 to 2005, *Geochem. Geophys. Geosyst.*, *7*, Q06008, doi:10.1029/2005GC001175.
Sadofsky, S. J., and G. E. Bebout (2004), Nitrogen geochemistry of subducting sediments: New results from the Izu-Bonin-Mariana margin and insights regarding global nitrogen subduction, *Geochem. Geophys. Geosyst.*, *5*, Q03115, doi:10.1029/2003GC000543.
Sano, Y., N. Takahata, G. Igarashi, N. Koizumi, and N. C. Sturchio (1998), Helium degassing related to the Kobe earthquake, *Chem. Geol.*, *150*, 171–179.
Schlindwein, V. (2012), Teleseismic earthquake swarms at ultraslow spreading ridges: Indicator for dyke intrusions?, *Geophys.J. Int.*, *190*, 442–456.
Siebenaller, L., M.-C. Boiron, O. Vanderhaeghe, C. Hibsch, M. W. Jessell, A.-S. Andre-Mayer, C. France-Lanord, and A. Photiades (2013), Fluid record of rock exhumation across the britte-ductile transition during formation of a Metamorphic Core Complex (Naxos Island, Cyclades, Greece), *J. Metamorph. Geol.*, *31*, 313–338.
Sigmundsson, F., P. Einarsson, S. T. Rögnvaldsson, G. R. Foulger, K. M. Hodgkinson, and G. Thorbergsson (1997), The 1994-1995 seismicity and deformation at the Hengill triple junction, Iceland: Triggering of earthquakes by minor magma injection in a zone of horizontal shear stress, *J. Geophys. Res.*, *102*, 15,151–15,161, doi:10.1029/97JB00892.
Sugisaki, R., and T. Sugiura (1986), Gas anomalies at three mineral springs and a fumarole before an inland earthquake, central Japan, *J. Geophys. Res.*, *91*, 12,296–12,304, doi:10.1029/JB091iB12p12296.
Sültenfuß, J., M. Rhein, and W. Roether (2009), The Bremen Mass Spectrometric Facility for the measurement of heliumisotopes, neon, and tritium in water, *Isotopes Environ. Health Stud.*, *45*, 1–13.
Torgersen, T., and J. O'Donnell (1991), The degassing flux from the solid earth: Release by fracturing, *Geophys. Res. Lett.*, *18*, 951–954, doi:10.1029/91GL00915.
Toutain, J. P., and J.-C. Baubron (1999), Gasgeochemistry and seismotectonics: A review, *Tectonophysics*, *304*, 1–27.
Tsunogai, U., and H. Wakita (1995), Precursory chemical changes in groundwater: Kobe earthquake Japan, *Science*, *269*, 61–62.
Van der Elst, N. J., H. M. Savage, K. M. Keranen, and G. A. Abers (2013), Enhanced remote earthquake triggering at fluid-injection sites in the Midwestern United States, *Science*, *341*, 164–167.
Weinlich, F. H., J. Tesař, S. M. Weise, K. Bräuer, and H. Kämpf (1998), Gas flux contribution in mineral springs and tectonic structure in the western Eger Rift, *J. Czech Geol. Soc.*, *43*, 91–110.
Weinlich, F. H., K. Bräuer, H. Kämpf, G. Strauch, J. Tesař, and S. M. Weise (1999), An active subcontinental mantle volatile system in the western Eger Rift, Central Europe: Gas flux, isotopic (He, C, N) and compositional fingerprints, *Geochim. Cosmochim. Acta*, *63*, 3653–3671.
Ziegler, P. A. (1992), European Cenozoic rift system, *Tectonophysics*, *208*, 91–111.